Vessels encapsulating tumor clusters type hepatocellular carcinoma: a distinct subtype with aggressive behavior

Ha Young Woo

Department of Medicine

The Graduate School, Yonsei University

Vessels encapsulating tumor clusters type hepatocellular carcinoma: a distinct subtype with aggressive behavior

Ha Young Woo

Department of Medicine

The Graduate School, Yonsei University

Vessels encapsulating tumor clusters type hepatocellular carcinoma: a distinct subtype with aggressive behavior

Directed by Professor Young Nyun Park

The Master's Thesis Doctoral Dissertation
submitted to the Department of Medicine,
the Graduate School of Yonsei University
in partial fulfillment of the requirements for the degree
of Doctor of Philosophy

Ha Young Woo

December 2020

This certifies that the Doctoral Dissertation of Ha Young Woo is approved.

Thesis Supervisor : Young Nyun Park

Thesis Committee Member#1 : Do Young Kim

Thesis Committee Member#2 : Jaemoon Yang

Thesis Committee Member#3: Hyun Goo Woo

Thesis Committee Member#4: Gi Hong Choi

The Graduate School
Yonsei University

December 2020

ACKNOWDEGMENETS

It is a great pleasure to express my deep sense of gratitude to my mentor Dr. Y.N.Park, Department of Pathology, Yonsei University College of Medicine. Her prompt inspiration, enthusiasm, meticulous scrutiny, scholarly advice and scientific approach have encouraged me to a very great extent to accomplish this task.

I express sincere gratitude to Dr. D.Y.Kim, Department of Internal Medicine, Yonsei University College of Medicine, J.M.Yang, Department of Radiology, Yonsei University College of Medicine, Dr. H.G.Woo, Department of Physiology, Ajou University School of Medicine, and Dr. G.H.Choi, Department of Surgery, Yonsei University College of Medicine whose guidance, suggestion and very constructive criticism have contributed immensely to the evolution of my research.

I would like to express my sincere gratitude to my precious colleagues in department of pathology, Yonsei University College of Medicine, who provided and encouraged a healthy research environment.

Finally, I am greatly grateful to my family and friends, for their constant encouragement throughout my research period.

<TABLE OF CONTENTS>

ABSTRACT ····· 1

I. INTRODUCTION ····· 4

II. MATERIALS AND METHOD ····· 6

1. Patients and samples ····· 6

2. Pathological examination ····· 7

3. Immunohistochemistry ····· 8

4. Statistical analysis ····· 11

III. RESULTS ····· 11

1. Clinical, pathological, and phenotypical features of VETC-HCC · 11

2. VETC is a distinct pathologic phenotype with aggressive biological behavior ····· 14

3. VETC is enriched in MTM subtype HCC ····· 22

4. Clinical, pathological, and phenotypical features according to molecular subgroups ····· 25

5. The TME of VETC-HCCs ····· 28

6. Survival analysis of each group ····· 33

7. Comparison of intrahepatic primary HCCs and extrahepatic metastatic HCCs ····· 34

A. Comparison of general pathological features and TME-related features of intrahepatic primary HCCs and extrahepatic metastatic HCCs ····· 35

B. Histological and immunohistochemical results among various

metastatic sites ·····38

C. Comparison of TME-related features in intrahepatic primary HCCs and their corresponding extrahepatic metastatic HCCs ·42

IV. DISCUSSION ·····45

V. CONCLUSION ·····47

REFERENCES ·····49

ABSTRACT (IN KOREAN) ·····53

LIST OF FIGURES

Figure 1. Flow diagram of case selection in each cohort ·····7
Figure 2. Representative images of vessels encapsulating tumor clusters ·····9
Figure 3. Kaplan-Meier curves of disease free survival, early recurrence, overall survival, and extrahepatic metastasis ·····22
Figure 4. Kaplan-Meier curves of disease free survival, early recurrence, overall survival, and extrahepatic metastasis ·····25
Figure 5. Clinicopathologic features associated with Wnt+ HCCs ·····28
Figure 6. Representative images of each group ·····31
Figure 7. Kaplan-Meier curves of disease free survival, early recurrence, overall survival, and extrahepatic metastasis ·····34
Figure 8. Representative images of extrahepatic metastatic HCCs at various metastatic sites ·····40
Figure 9. Comparison of various phenotypic features in matched pairs of primary and metastatic HCCs·····44

LIST OF TABLES

Table 1. Antibodies, sources, clones, dilutions and interpretation criteria for immunohistochemistry ·····10
Table 2. Clinicopathologic characteristics of HCC patients ·····13
Table 3. Comparison of clinicopathological features of VETC-HCC and non-VETC-HCC·····16
Table 4. Univariable and multivariable analysis on early recurrence····17
Table 5. Univariable and multivariable analysis on disease-free survival ·····18

Table 6. Univariable and multivariable analysis on overall survival ····19
Table 7. Univariable and multivariable analysis on extrahepatic metastasis ····20
Table 8. Comparison of clinicopathological features of MTM and non-MTM-HCC ····23
Table 9. Comparison of clinicopathological features of p53+ HCC and non-p53+ HCC ····26
Table 10. Comparison of clinicopathological features of Wnt+ HCC and non-Wnt+ HCC ····27
Table 11. Comparison of TME-related features of VETC-HCCs and non-VETC-HCCs ····29
Table 12. Comparison of TME-related features in each group ····32
Table 13. Baseline characteristics of the extrahepatic metastatic HCCs (cohort 2, n=130) ····35
Table 14. Comparison of general pathological and TME-related features between primary and extrahepatic metastatic HCC ····36
Table 15. Comparison of extrahepatic metastatic HCCs according to EMT signature ····38
Table 16. Comparison of extrahepatic metastatic HCCs among different metastatic sites ····33

ABSTRACT

Vessels encapsulating tumor clusters type hepatocellular carcinoma: a distinct subtype with aggressive behavior

Ha Young Woo

Department of Medicine,
The Graduate School, Yonsei University

(Directed by Professor Young Nyun Park)

Hepatocellular carcinoma (HCC) is one of the leading causes of cancer death worldwide. The concept of tumor microenvironment (TME) has been established as an integrated and essential component of the cancer development and progression. Among the heterogeneous population comprising TME, endothelial cells in HCC are of particular interest because they are strikingly involved in the tumor growth and represent a potential therapeutic target (transarterial chemoembolization, drugs). Recently, Fang et al. reported a distinct pattern of HCC vascularization that predicted rapid tumor dissemination and high recurrence rates. This pattern is characterized by the presence of CD34+ vessels completely encapsulating tumor clusters (VETC). In this study, we tried to refine the clinico-pathological features of VETC phenotype, especially in terms of TME.

This study was performed on surgically resected primary liver (cohort 1, n=322) and extrahepatic metastatic (cohort 2, n=130) HCC tissue samples, obtained from Severance Hospital (Seoul, Korea), from 2006 to 2012. The tissue microarray was constructed, of which 96 cases of cohort 1 were stained with CD34 in the whole sections. The full spectrum of clinical and pathological variables was collected and fibrous tumor stroma and immune cell infiltration was assessed in each tumor. The following immunostaining

was performed: tumor vessel (CD34), cancer-associated fibroblast (αSMA, FAP), tumor-associated macrophage (CD163), epithelial-mesenchymal transition (EMT; Zebl, IL-6, Snail, Ezrin, S100A4, E-cadherin), tumor immunity (PD-L1), hypoxia (CAIX), stemness (K19), molecular phenotypic markers (p53, glutamine synthetase, and β-catenin).

The VETC phenotype (defined as ≥ 55% tumor area by CD34 immunostaining) was easily reproducible and reliably detectable in whole sections and small-sized tissues of tissue microarray. VETC-HCCs represented 23.0% of the cases and was significantly associated with several clinical and pathological features such as high alpha-fetoprotein (AFP) and PIVKA-II level, tumor size greater than 5 cm, macrovascular invasion, poor differentiation, macrotrabecular pattern, frequent microvascular invasion, multinucleated cells ($p<0.05$ for all). VETC phenotype was associated with early recurrence (HR 1.91 [1.20-3.02]; p=0.006), shorter DFS (HR 1.55 [1.07-2.24]; p=0.233), OS (HR 2.84 [1.29-6.26]; p=0.010), and extrahepatic metastasis (HR 2.38 [1.21-4.64]; p=0.011), in multivariable analysis. This distinct vascular pattern was enriched in the macrotrabecular massive HCC subtype, which was seen in 10.6% of patients. The VETC pattern was found to be easily detectable and a powerful pathological finding affecting survival.

In terms of TME, VETC-HCCs showed less immune cell infiltration, scarce fibrous stroma, less PD-L1 expression, and increased CAIX expression. As non-VETC type HCCs, which are 77.0% of HCCs, had heterogenous TME, we further divided into groups of VETC-HCCs (n=74), non-VETC-HCCs with (n=117) or without fibrous stroma (n=131). Non-VETC type HCCs with fibrous stroma showed higher frequency of EMT-high, K19 expression, rich immune cell infiltration, PD-L1 expression, and double negative phenotype, compared to other groups. Non-VETC type HCCs without fibrous stroma showed similar level of K19 expression, macrophage infiltration and PD-L1 expression compared to VETC type HCC and higher frequency of p53 phenotype than Non-VETC type HCCs with fibrous stroma.

On survival analysis, overall, the patients with VETC-HCC had the worst outcome, patients with non-VETC-HCCs without fibrous tumor stroma had

the best prognosis, patients with non-VETC-HCCs with fibrous tumor were in the middle.

Extrahepatic metastatic HCCs demonstrated more MTM subtype with CAIX expression and EMT-high and K19-expressing TME, than intrahepatic primary HCCs. Extrahepatic metastatic HCCs with EMT-low group (74%) were associated with VETC type HCCs. Extrahepatic metastatic HCCs with EMT-high group (26%) were associated with abundant fibrous stroma, K19 expression, rich immune cell infiltration and high level of PD-L1 expression. The metastatic tumors in lungs are associated with MTM subtype with VETC type HCCs. The metastatic tumors in LNs are more likely to express stemness- and EMT- related markers and PD-L1. In analysis for matched pair of primary and metastasis, overall, various features of HCCs including VETC were conserved during metastasis. This study suggests that VETC phenotype is a distinct aggressive subtype with CAIX expression, EMT-low TME, and may predict response to immune checkpoint inhibitors.

Key words: Hepatocellular carcinoma, vessels encapsulating tumor cluster, tumor microenvironment, epithelial-mesenchymal transition, molecular classification

Vessels encapsulating tumor clusters type hepatocellular carcinoma: a distinct subtype with aggressive behavior

Ha Young Woo

Department of Medicine,
The Graduate School, Yonsei University

(Directed by Professor Young Nyun Park)

I. INTRODUCTION

Hepatocellular carcinoma (HCC) is one of the leading causes of cancer death worldwide, and its incidence is particularly high in Asian countries[1,2]. HCC tumorigenesis is a complex multistep process, with 70-80% of cases developed in the clinical context of chronic liver disease and liver cirrhosis[3,4]. The process starts with pre-cancerous cirrhotic nodules (i.e. dysplastic nodules), which might eventually convert into overt HCC.

In last decades, integrative molecular analyses including genomic, transcriptomic, and epigenomic profiling of HCCs have been evolved and provided the fundamental concept of the molecular classification of HCC subtypes[5-9]. Notably, recent studies have reported that 'cold' tumors defined by WNT/CTNNB1 mutations are predictive to primary resistance to immune checkpoint inhibitors[10-13], implying that exploring molecular subtype can provide important clues to the clinical management of HCC.

The concept of tumor microenvironment (TME) has been established as an integrated and essential component of the cancer development and progression[14,15]. The TME has many components, including tumor cells, stroma, a tumor-friendly immune environment, a special modified metabolism, invasive epithelial-mesenchymal transition (EMT) phenotype, and tumor stem cell compartment. Among this heterogeneous population, endothelial cells in HCC are of particular interest because they are strikingly involved in the tumor growth and represent a potential therapeutic target (transarterial chemoembolization [TACE], drugs). Intratumoral endothelial cells

progressively lose sinusoidal markers, including stabilin-1, stabilin-2, LYVE-1 (lymphatic vessel endothelial hyaluronan receptor 1), CD32 (cluster of differentiation 32/34), and ICAM (intercellular adhesion molecule)[16]; at the same time, they gain markers of continuous, nonfenestrated endothelial cells (i.e., capillary), such as CD34[17,18]. Accordingly, the process of pathological angiogenesis in HCC is mostly known as capillarization. Recently, it has been investigated that sinusoidal capillarization and angiogenesis is closely related to HCC progression[19,20]. As in many other solid tumors, once angiogenesis is completed, HCC is more prone to progress and to metastasize. Moreover, a shift from a "dormant" angiogenesis that supports tumor growth, but not metastases, to an "active" more aggressive, pro-metastatic angiogenesis has been postulated in many organs[21,22]. It is therefore likely that vascular pattern heterogeneity can also play a role in tumor progression[23]. Moreover, Fang et al. reported a distinct pattern of HCC vascularization that predicted rapid tumor dissemination and high recurrence rates[24]. This pattern is characterized by the presence of CD34+ vessels completely encapsulating tumor clusters (VETC). Although conducted in a limited HCC population (hepatitis B virus [HBV]-related and >5 cm), the authors elegantly showed VETC clusters delivering tumor emboli into larger vessels. Moreover, the same authors recently claimed sorafenib therapy to be more effective in VETC HCC[25].

The extrahepatic metastasis occurs in 14.0–36.7% of patients with HCC[26], is still regarded as a terminal event, as it not only limits the treatment option for HCC, but also is the main cause of liver and organ failure. The cancer stemness has been considered as one of the most important component for initiation of metastasis[27,28]. However, Fang et al[24] suggested that this VETC phenotype is not associated with EMT, indicating that EMT alone is not sufficient to tumor metastasis.

In this study, we collected a large series of HCC patients to investigate the clinical impact of VETC pattern. We tried to assess the biological characteristics of VETC in terms of TME. Moreover, we analyzed various pathological features of HCCs before and after extrahepatic metastasis. This is, to our knowledge, the first study to compare the pathological features,

especially including TME-related features of primary liver HCC and extrahepatic metastatic HCCs in a relatively large number of patients.

II. MATERIALS AND METHODS

1. Patients and samples

This study was performed on surgically resected primary liver (cohort 1, n=322) and extrahepatic metastatic (cohort 2, n=130) HCC tissue samples, obtained from Severance Hospital (Seoul, Korea), from 2006 to 2013. Only cases staged R0 after surgical resection were included in the study.

The clinical outcomes of the patients were collected retrospectively by reviewing the electronic medical records. The endpoints were defined as follows: Overall survival (OS) was defined by the interval between surgery and death regardless of cause; and disease-free survival (DFS) was defined as the time from surgery to an initial diagnosis of recurrence regardless of location. The mean follow-up duration was 50 months. The study protocol conforms to the ethical guidelines of the 1975 Declaration of Helsinki, as reflected in a priori approval by the institution's human research committee. This study was approved by the institutional review boards of Severance hospital (4-2018-0409, 2016-2797-001), and the requirement for informed consent was waived. The following clinical features were systematically recorded: age, gender, etiology of chronic liver disease (hepatitis B virus [HBV], hepatitis C virus [HCV], alcohol intake, other), pre-operative serum levels of alpha-fetoprotein (AFP) and protein induced by vitamin K absence-II (PIVKA-II). Staging according to the Barcelona Clinic of Liver Cancer (BCLC) system was also available.

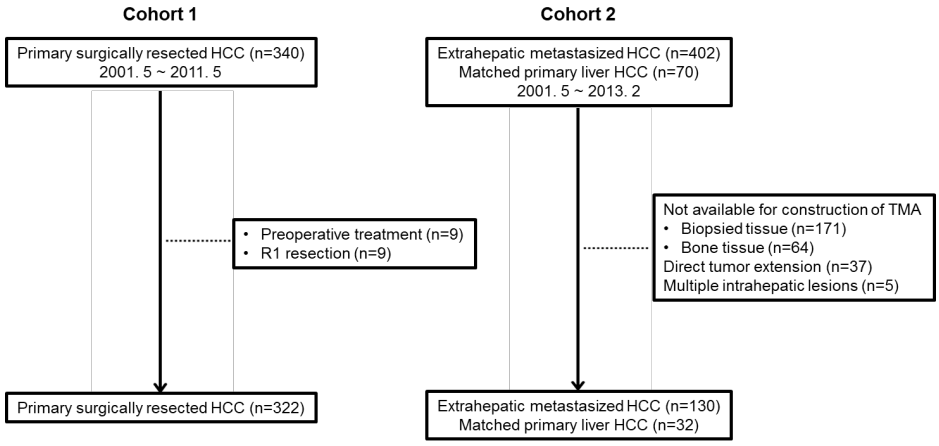

Figure 1. Flow diagram of case selection in each cohort

2. Pathological examination

The following features were analyzed regarding the general macroscopic characteristics: tumor size, multiplicity, and macrovascular invasion. For evaluating microscopic pathological parameters, at least one representative section was available for each case. The following general microscopic variables were analyzed: tumor grade (according to Edmondson-Steiner); pattern of growth (at least 20% of the tumor area: microtrabecular, macrotrabecular, compact, or pseudoglandular); microvascular invasion; tumor capsule; tumor fibrous stroma (fibrous band intervening tumor nests≥20% of tumor area) and cirrhosis of the surrounding liver parenchyma. Moreover, the following tumoral cytological findings were recorded: cholestasis, clear, multinucleate and pleomorphic cells, sarcomatous changes, and hyaline bodies. The tumor subtype (scirrhous, lymphoepithelioma-like, sarcomatoid, steatohepatitic, and the recently described macrotrabecular massive [MTM] subtype[29,30], the latter in at least 50% tumor area) was recorded. The degree of immune cell infiltration was assessed according to the proposed guidelines for the assessment of tumor-infiltrating lymphocytes (TILs) in solid tumor: recommendations by an International Immuno-Oncology Biomarkers Working Group[31]. Mononuclear cells in intra-tumoral/stromal compartment at central tumor and invasive margin area

were semi-quantitatively evaluated. High immune cell infiltration was defined as mononuclear cells ≥10% of surface area or density of tertiary lymphoid stroma (TLS)≥5 foci.

All available histological slides were reviewed by 2 expert liver pathologists (H.Y.W. and Y.N.P.), who were blinded to the clinical data.

3. Immunohistochemistry

Tissue microarrays (TMAs; two different tumoral cores for each case, diameter ranging from 2-3mm) were constructed from the surgical specimens of cohort 1 and cohort 2.

Immunohistochemical stain was performed using an automated staining system (Discovery XT; Ventana Medical Systems, Oro Valley, AZ) according to the manufacturer's instructions; antibodies, sources, clones, dilutions, and interpretation criteria are detailed in Table 1. Membranous and/or cytoplasmic immunoreactivity was evaluated using H-score method, obtained by multiplying intensity (0, no detectable staining; 1, weak reactivity mainly detectable at high magnification [20-40x objective]; 2, moderate reactivity; 3, intense reactivity easily detectable at low magnification [4x objective]) and the extent of staining area (%). Regarding CD34 evaluation, unequivocal immunoreactivity of a continuous lining around tumor clusters was defined as VETC, and the area of VETC was semi-quantitatively evaluated from 0% to 100% in 5% units. This VETC pattern was considered alternative to the other common capillary pattern, sustained by the growth of small circular vessels. Both patterns are illustrated in Figure 2. To check the correlation between the VETC of whole sectioned slides and that of TMAs, an immunohistochemical stain for CD34 was performed in matched whole sections and the TMAs of 96 HCCs.

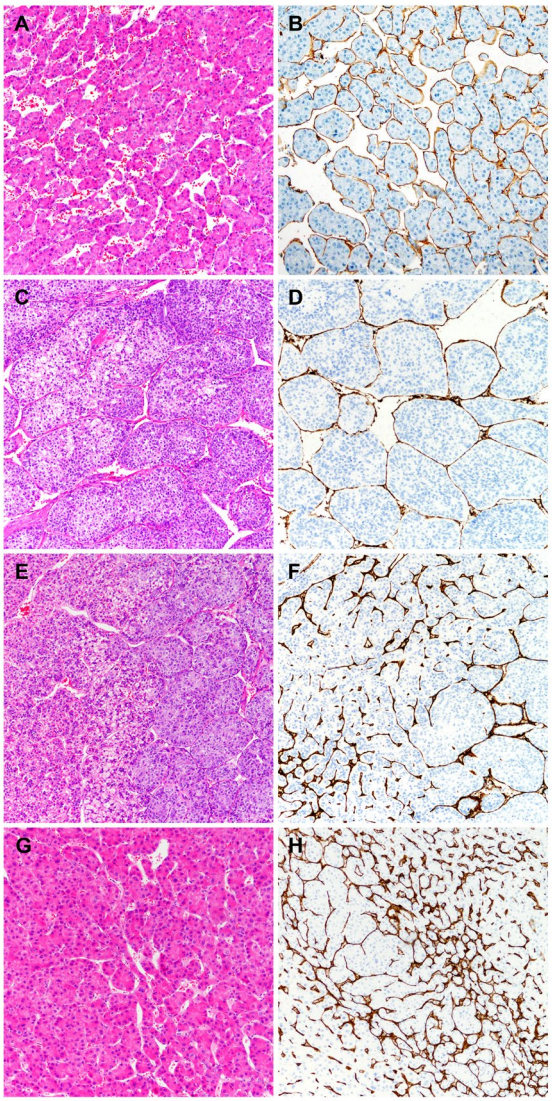

Figure 2. Representative images of vessels encapsulating tumor clusters (VETC). VETC seen in micro- (A and B) and macro- (C and D) trabecular patterns of growth. Panel A and B shows tumor cell clusters encapsulated by CD34-positive endothelial cells of 3-4 cells in thickness. Panel C and D shows VETC of more than 6 cells in thickness. Panels E-H illustrate different proportion of VETC features and capillary pattern (Left panel: Hematoxylin&eosin stain; right panel: CD34 immunohistochemical stain, 100x magnification).

Table 1. Antibodies, sources, clones, dilutions and interpretation criteria for immunohistochemisty

Antibody	Source	Clone	Dilution	Interpretation criteria
CD34	Ventana (Tucson, AZ, USA)	QBEnd/10	Pre-diluted	Membranous expression, described in the text
Glutamine synthetase	Ventana (Tucson, AZ, USA)	GS-6	Pre-diluted	Cytoplasmic expression, diffuse
p53	Ventana (Tucson, AZ, USA)	DO-7	Pre-diluted	Nuclear expression, ≥50%
β-catenin	Ventana (Tucson, AZ, USA)	14	Pre-diluted	Nuclear expression, any
CK19	Dako (Glostrup, Denmark)	RCK108	1:25	Cytoplasmic/membranous expression, ≥5%
CAIX	Abcam (Cambridge, UK)	ab15086	1:2000	Cytoplasmic/membranous expression, ≥5%
EpCAM	Calbiochem (Darmstadt, Germany)	VU-1D9	1:1000	Cytoplasmic/membranous expression, ≥5%
α-SMA	Dako (Glostrup, Denmark)	1A4	1:1000	Cytoplasmic expression, ≥20% of tumor area
FAP	Vitatex (Stony Brook, NY, USA)	Seprase D8	1:100	Cytoplasmic expression, ≥5% of tumor area
Ezrin	Abcam (Cambridge, UK)	3C12	1:100	Cytoplasmic expression, H-score≥100
E-Cadherin	Dako (Glostrup, Denmark)	NCH-38	Pre-diluted	Membranous expression, H-score≤50
S100A4	Abcam (Cambridge, UK)	ab41532	Pre-diluted	Cytoplasmic expression, H-score≥100
Snail	Abcam (Cambridge, UK)	ab85936	Pre-diluted	Nuclear expression, ≥5%
Zeb1	Cell Signaling Technology (Beverly, MA, USA)	D80D3	1:50	Nuclear expression, ≥5%
PD-L1	Cell Signaling Technology (Beverly, MA, USA)	E1L3N	1:100	Cytoplasmic/membranous expression, Tumor: ≥1% of tumor cells; immune cell: ≥5 clusters/10 HPF
CD163	Cell Marque (Rocklin, California)	MRQ-26	1:50	Cytoplasmic expression, ≥5% of tumor area

4. Statistical analysis

Categorical variables were compared using the $\chi 2$ test or Fisher's exact test. Kaplan-Meier survival curves and log-rank statistics were used to evaluate the time to early (≤2 years) or late (>2 years) recurrence and OS. Multivariable regression analysis was performed using the Cox proportional hazards model. After we confirmed that VETC is a meaningful prognostic factor as a continuous variable, we used the K-adaptive partitioning algorithm to find the point at which the log-rank statistics are maximized and obtained the optimal cutoff value. The intraclass correlation coefficient was used to compare the VETC (%) of surgical specimens and TMAs in 96 cases, and the Cohen' kappa value was used to compare the agreement of the 2 reviewers (H.Y.W., Y.N.P.) in 60 cases. All values were considered to be good agreement when it was 0.6 or more. Two-sided paired McNemar's test was used to evaluate the concordance of phenotypic features between matched pairs of primary and metastatic lesions and among the multiple metastatic lesions. For analyzing data with multiple comparisons, we used the Bonferroni correction to generate adjusted p-value.

All statistical analyses were performed using SPSS software (version 21.0; IBM Statistics, Armonk, NY) and R software (version 3.5.1 for Windows; the R foundation for statistical computing, Vienna, Austria). All statistical tests were two-tailed; $P < 0.05$ was considered statistically significant.

III. RESULTS

1. Clinical, pathological, and phenotypical features of VETC-HCC

The baseline clinico-pathologic features of the cohort 1 is summarized in Table 1. There was a strong male predominance (259/322, 80.4%) and the most of the cases were related to HBV infection (265/322, 82.3%) and rarely to HCV infection (18/322, 5.6%) and alcohol intake (15/322, 4.7%). The majority of the cases were BCLC 0/A (294/322, 91.3%), single masses (285/322, 88.5%) and 5 cm or less (258/322, 80.1%). The most common gross morphology was expanding (161/322, 50.0%), followed by multinodular

confluent (100/322, 31.1%), nodular with perinodular extension (36/322, 11.2%), infiltrative (17/322, 5.3%), and vaguely nodular (8/322, 2.5%). Poorly differentiated HCCs (Edmondson grade III-IV) were observed in 56.5% (182/322).

Various architectural patterns and cytological features were observed in each case: microtrabecular, macrotrabecular, pseudoglandular, and compact patterns were recorded in 87.6%, 49.4%, 35.7%, and 32.6% of the tumors, respectively. MTM HCC was the most frequent subtype identified (34/322, 10.6%), followed by steatohepatitic (7/322, 2.2%), scirrhous (1.5%), lymphoepithelioma-like (3/322, 0.9%), scirrhous (3/322, 0.9%), and sarcomatoid (1/322, 0.3%) subtype.

HCCs were further classified according to the following molecular phenotypes: p53+ and β-catenin/GS- (briefly, p53+) 29.1% (91/313); p53- and β-catenin/GS+ (briefly, β-catenin/GS+) 17.3% (54/313); p53+ and β-catenin/GS+ (briefly, double positive) 2.6% (8/313); and p53- and β-catenin/GS- (briefly, double negative) 51.1% (160/313).

Clinical follow-up data were available for 336 patients: Cancer-related death, extrahepatic metastasis and recurrence occurred in 10.9% (35/322), 16.1% (52/322) and 44.1% (142/322) of HCC patients, respectively. Early (≤2 years) and late (>2 years) recurrence was observed in 30.1% (97/322) and 14.0% (45/322) of HCC in the whole cases.

Table 2. Clinicopathologic characteristics of HCC patients

Variables	Available data (n)	n (%)
Clinical features		
Age (> 60 years)	322	107 (33.2)
Gender (male/female)	322	259 (80.4)/63 (19.6)
Etiology (HBV/HCV/Alcohol/Undetermined)	322	265 (82.3)/18 (5.6)/15 (4.7)/24 (7.5)
BCLC (0/A/B/C)	322	37 (11.5)/257 (79.8)/28 (8.7)/0 (0.0)
Serum AFP > 400 ng/ml	321	66 (20.6)
Serum PIVKA-II > 300 mAU/mL	321	94 (29.2)
Macroscopic general pathological features	322	
Tumor size > 5 cm		64 (19.9)
Multiplicity		37 (11.5)
Macrovascular invasion		13 (4.0)
Gross morphology		
Vaguely nodular		8 (2.5)
Expanding		161 (50.0)
Nodular with perinodular extension		36 (11.2)
Multinodular confluent		100 (31.1)
Infiltrative		17 (5.3)
Microscopic general pathological features	322	
Edmondson grade III-IV		182 (56.5)
Architectural pattern		
Microtrabecular		282 (87.6)
Macrotrabecular		159 (49.4)
Pseudoglandular		115 (35.7)
Compact		105 (32.6)
Microvascular invasion		186 (57.8)
Capsule infiltration		66 (20.5)
Cirrhosis of background liver		174 (54.0)
Tumoral cytological findings	322	
Tumoral cholestasis		45 (14.0)
Clear cells		95 (29.5)
Pleomorphic cells		82 (25.5)
Multinucleate cells		102 (31.7)
Sarcomatous change		2 (0.6)
Hyaline bodies		41 (12.7)
Tumoral variants	322	
Scirrhous		3 (0.9)
Lymphoepithelioma-like		3 (0.9)
Sarcomatoid		1 (0.3)
Steatohepatitic		7 (2.2)
Macrotrabecular-massive		34 (10.6)
Molecular phenotype[1]	313	
p53+		91 (29.1)

β-catenin,GS+		54 (17.3)
positive		8 (2.6)
Double negative		160 (51.1)
Follow up	322	
Non-survivor		35 (10.9)
Extrahepatic metastasis		52 (16.1)
Recurrence		142 (44.1)
Early recurrence (≤ 2 year)		97 (30.1)
Late recurrence (> 2 year)		45 (14.0)

[1]p53+: p53+ and βcatenin/GS-; βcatenin/GS+: p53- and βcatenin/GS+; double positive: p53+ and βcatenin/GS+; double negative: p53- and βcatenin/GS-

2. VETC is a distinct pathologic phenotype with aggressive biological behavior

The degree of VETC area ranged from 0% to 100% of the tumor surface. The reliability between VETC of whole sectioned slides and that of TMA was evaluated in 96 matched cases, and it was good (intraclass correlation coefficient [95% confidence interval (CI): 0.642] 0.489-0.733); then VETC was evaluated in a total of 322 HCCs using TMA. At least 5% VETC tumor area was seen in 53.4% (172/322) of HCCs, and the median value of VETC was 5% (Q1-Q3, 0%-50%). Multivariable cox regression analysis with the collected parameters confirmed that VETC, evaluated in 5% unit, was a meaningful prognostic factor. VETC was significantly associated with poorer DFS, early relapse, overall survival, and extrahepatic metastasis (DFS HR: 1.04 [1.01-1.08]; p=0.006; early relapse HR: 1.04 [1.01-1.08]; p=0.006; OS HR: 1.06 [1.00-1.11]; p=0.041; extrahepatic metastasis HR: 1.06 [1.01-1.11]; p= 0.009) at multivariable analysis. By using K-adaptive partitioning algorithm, we set a value of 55% as the optimal cutoff value of VETC phenotype to predict prognosis. By applying the cutoff value of VETC 55%, HCCs were classified into VETC-HCC and non-VETC-HCC. The agreement of the VETC phenotype among 2 pathologists (H.Y.W., and Y.N.P.) was good (Cohen's kappa value [95% CI]: 0.879 [0.784-0.991]).

The VETC phenotype (≥55%) was observed in 23.0% (74/322) of HCCs and associated with several aggressive clinicopathological features: high

serum levels of AFP (>400 ng/mL, 32.9% and 16.9%, p=0.005) and PIVKA-II (>300 mAU/mL, 51.4% and 22.6%, p<0.001); larger tumor size (>5 cm, 32.4% and 16.1%, p=0.003); macrovascular invasion (9.5% and 2.4%, p=0.014); Edmondson grade III-IV (77.0% and 50.4%, p<0.001); macrotrabecular pattern (81.1% and 39.9%, p<0.001); microvascular invasion (78.4% and 51.6%, p<0.001) and multinucleated cells (45.9% and 27.4%, p=0.004). The VETC phenotype was not correlated with any specific gross morphology. Interestingly, we found that MTM subtype, which has been proposed as a morphologic subtype with poor prognosis, was obviously associated with VETC-HCC (25.7% and 6.0%, p<0.001).

For molecular phenotypic markers, in VETC-HCC, β-catenin/GS+ (37.7%) was the most common subgroup, followed by double negative (36.2%), p53+ (23.2%), and double positive (2.9%). In contrast, in non-VETC HCC, double negative subgroup (55.3%) occupied the majority of the tumors, followed by p53+ (30.7%), β-catenin/GS+ (11.5%), and double positive (2.5%). VETC HCC was clearly enriched in β-catenin/GS+ group (p<0.001) and impoverished in double negative group (p=0.006) (Table 3).

VETC phenotype was associated with earlier recurrence, poorer DFS, OS and frequent extrahepatic metastasis, compared with non-VETC HCC (p<0.05 for all) (Fig. 2). The significant clinical impact of VETC phenotype was confirmed at multivariable analysis for early recurrence (HR 1.91 [1.20-3.02]; p=0.006), OS (HR 2.84 [1.29-6.26]; p=0.010), and extrahepatic metastasis (HR 2.38 [1.21-4.64]; p=0.011), but not for DFS (HR 1.31 [0.84-2.03]; p=0.233) (Table 3-6).

Table 3. Comparison of clinicopathological features of VETC-HCC and non-VETC-HCC

Variables	Non-VETC-HCC (n=248, n [%])	VETC-HCC (n=74, n [%])	p-value
Clinical features			
Age (> 60 years)	80 (32.3)	27 (36.5)	0.340
Male gender	201 (81.0)	58 (78.4)	0.619
Etiology			
HBV infection	205 (82.7)	60 (81.1)	0.755
HCV infection	13 (5.2)	5 (6.8)	0.574
Alcohol intake	10 (4.0)	5 (6.8)	0.348
BCLC stage B-C	18 (7.3)	10 (13.5)	0.103
Serum AFP > 400 ng/ml	42 (16.9)	24 (32.9)	0.005
Serum PIVKA-II >300mAU/mL	56 (22.6)	38 (51.4)	<0.001
Macroscopic pathological features			
Tumor size > 5 cm	40 (16.1)	24 (32.4)	0.004
Multiplicity	27 (10..9)	10 (13.5)	0.536
Macrovascular invasion	6 (2.4)	7 (9.5)	0.014
Gross morphology			
Vaguely nodular	8 (3.2)	0 (0.0)	0.206
Expanding	119 (48.0)	42 (56.8)	0.233
Nodular with perinodular extension	26 (10.5)	10 (13.5)	0.528
Multinodular confluent	82 (33.1)	18 (24.3)	0.197
Infiltrative	13 (5.2)	4 (5.4)	1.000
Microscopic pathological features			
Edmondson grade III-IV	125 (50.4)	57 (77.0)	<0.001
Architectural pattern			
Microtrabecular	216 (87.1)	66 (89.2)	0.841
Macrotrabecular	99 (39.9)	60 (81.1)	<0.001
Pseudoglandular	82 (33.1)	33 (44.6)	0.074
Compact	84 (33.9)	21 (28.4)	0.400
Microvascular invasion	128 (51.6)	58 (78.4)	<0.001
Capsule infiltration	46 (18.5)	20 (27.0)	0.139
Cirrhosis	131 (52.8)	43 (58.1)	0.507
Tumoral cytological findings			
Tumoral cholestasis	31 (12.5)	14 (18.9)	0.182
Clear cells	70 (28.2)	25 (33.8)	0.385
Pleomorphic cells	57 (23.0)	25 (33.8)	0.069
Multinucleate cells	68 (27.4)	34 (45.9)	0.004
Sarcomatous change	2 (0.8)	0 (0.0)	1.000
Hyaline bodies	31 (12.5)	10 (13.5)	0.843
Tumoral variants			
Scirrhous	3 (1.2)	0 (0.0)	1.000
Lymphoepithelioma-like	3 (1.2)	0 (0.0)	1.000
Sarcomatoid	1 (0.4)	0 (0.0)	1.000
Steatohepatitic	7 (2.8)	0 (0.0)	0.359

Macrotrabecular-massive	15 (6.0)	19 (25.7)	<0.001
Molecular phenotype[1]			
p53+	75 (30.7)	16 (23.2)	0.293
β-catenin,GS+	28 (11.5)	26 (37.7)	<0.001
Double positive	6 (2.5)	2 (2.9)	1.000
Double negative	135 (55.3)	25 (36.2)	0.006

VETC, vessel encapsulating tumor clusters; MTM, macrotrabecular-massive subtype

[1]p53+: p53+ and βcatenin/GS-; βcatenin/GS+: p53- and βcatenin/GS+; double positive: p53+ and βcatenin/GS+; double negative: p53- and βcatenin/GS-

Table 4. Univariable and multivariable analysis on early recurrence

Variables	Early recurrence			
	HR (95% CI)	P value	HR (95% CI)	P value
Clinical features				
Age>60 years	1.13 (0.75-1.70)	0.532		
Male sex	0.99 (0.43-2.03)	0.745		
HBV infection	0.84 (0.52-1.36)	0.496		
HCV infection	1.34 (0.62-2.89)	0.450		
BCLC stage B-C	2.61 (1.58-4.30)	<0.001	1.06 (0.35-3.22)	0.920
AFP>400 ng/ml	1.12 (0.70-1.78)	0.626		
PIVKA-II>300mAU/mL	1.62 (1.07-2.44)	0.022	0.93 (0.54-1.59)	0.787
General macroscopic				
Tumor size > 5 cm	2.00 (1.32-3.04)	0.001	1.27 (0.74-2.19)	0.390
Multiplicity	2.29 (1.43-3.67)	0.001	1.67 (0.99-2.81)	0.053
Macrovascular invasion	4.04 (2.10-7.79)	<0.001	5.18 (2.41-11.17)	<0.001
General microscopic				
Edmondson grade III-IV	1.93 (1.26-2.95)	0.002	1.22 (0.73-2.02)	0.446
Microtrabecular	1.03 (0.57-1.84)	0.917		
Macrotrabecular	1.80 (1.20-2.69)	0.004	1.38 (0.83-2.31)	0.214
Pseudoglandular	0.62 (0.39-0.97)	0.038	1.03 (0.66-1.62)	0.889
Compact	1.05 (0.70-1.57)	0.805		
Microvascular invasion	2.48 (1.58-3.90)	<0.001	1.89 (1.16-8.09)	0.012
Capsule infiltration	1.17 (0.75-1.84)	0.479		
Cirrhosis	1.38 (0.93-2.05)	0.108		
Tumoral cytological findings				
Tumoral cholestasis	0.67 (0.37-1.83)	0.145		
Clear cells	1.00 (0.65-1.53)	0.982		
Pleomorphic cells	1.23 (0.80-1.89)	0.330		
Multinucleated cells	1.21 (0.80-1.84)	0.371		
Hyaline bodies	0.71 (0.37-1.37)	0.312		
Tumoral variants				
Scirrhous	2.27 (0.56-9.21)	0.252		
Lymphoepithelioma-like	0.05	0.474		

	(0.00-189.54)			
Sarcomatoid	158.33 (14.36-946.13)	<0.001	-	-
Steatohepatitic	0.94 (0.23-3.81)	0.931		
Macrotrabecular-massive	1.13 (0.62-2.07)	0.680		
Phenotypic markers				
VETC	1.77 (1.15-2.72)	0.009	1.91 (1.20-3.02)	0.006
Molecular phenotype[1]				
p53+	1.08 (0.63-1.62)	0.794		
β-catenin/GS+	1.34 (0.78-2.64)	0.304		
Double positive	0.05 (0.00-78.28)	0.247		
Double negative	0.92 (0.61-1.48)	0.700		

VETC, vessel encapsulating tumor clusters
[1]p53+: p53+ and βcatenin/GS-; βcatenin/GS+: p53- and βcatenin/GS+; double positive: p53+ and βcatenin/GS+; double negative: p53- and βcatenin/GS-

Table 5. Univariable and multivariable analysis on disease-free survival

Variables	Disease-free survival			
	HR (95% CI)	P value	HR (95% CI)	P value
Clinical features				
Age>60 years	0.65 (0.35-1.45)	0.206		
Male sex	1.09 (0.52-2.12)	0.946		
HBV infection	1.48 (0.60-2.48)	0.228		
HCV infection	1.52 (0.71-2.46)	0.706		
BCLC stage B-C	2.89 (1.87-4.52)	<0.001	1.03 (0.50-2.11)	0.906
AFP>400ng/ml	1.20 (0.89-2.15)	0.413		
PIVKA-II>300mAU/mL	1.53 (0.99-2.27)	0.008	1.50 (1.04-2.17)	0.030
General macroscopic				
Tumor size > 5 cm	1.91 (1.32-2.70)	0.001	1.37 (1.03-2.09)	0.141
Multiplicity	2.02 (1.23-3.04)	0.002	1.45 (0.79-2.64)	0.228
Macrovascular invasion	4.15 (2.23-7.65)	<0.001	3.47 (1.78-6.79)	<0.001
General microscopic				
Edmondson grade III-IV	1.76 (1.23-2.44)	0.002	1.23 (0.82-2.75)	0.310
Microtrabecular	0.80 (0.58-1.21)	0.456		
Macrotrabecular	1.53 (0.99-2.09)	0.017	1.02 (0.67-1.56)	0.919
Pseudoglandular	0.72 (0.39-1.12)	0.516		
Compact	0.77 (0.51-1.16)	0.176		
Microvascular invasion	2.02 (1.40-2.99)	<0.001	1.41 (1.03-2.73)	0.019
Capsule infiltration	1.05 (0.62-2.25)	0.852		
Cirrhosis	1.73 (0.96-2.54)	0.002	2.01 (1.40-2.87)	<0.001
Tumoral cytological findings				
Tumoral cholestasis	0.70 (0.42-1.65)	0.117		
Clear cells	0.98 (0.77-1.67)	0.746		
Pleomorphic cells	1.12 (0.74-1.92)	0.179		

Multinucleated cells	1.85 (1.04-3.28)	0.135		
Hyaline bodies	1.99 (1.39-2.49)	0.275		
Tumoral variants				
Scirrhous	1.64 (0.40-6.64)	0.487		
Lymphoepithelioma-like	0.64 (0.09-4.63)	0.665		
Sarcomatoid	158.33 (14.35-946.12)	<0.001	203.05 (17.47-959.55)	<0.001
Steatohepatitic	0.99 (0.32-3.11)	0.986		
Macrotrabecular-massive	1.32 (0.81-2.16)	0.271		
Phenotypic markers				
VETC	1.94 (1.37-2.75)	<0.001	1.55 (1.07-2.24)	0.021
Molecular phenotype[1]				
p53+	0.88 (0.59-1.29)	0.515		
β-catenin/GS+	1.32 (0.87-2.41)	0.188		
Double positive	0.21 (0.03-1.52)	0.123		
Double negative	1.04 (0.61-1.78)	0.822		

VETC, vessel encapsulating tumor clusters
[1]p53+: p53+ and βcatenin/GS-; βcatenin/GS+: p53- and βcatenin/GS+; double positive: p53+ and βcatenin/GS+; double negative: p53- and βcatenin/GS-

Table 6. Univariable and multivariable analysis on overall survival

Variables	Overall survival			
	HR (95% CI)	P value	HR (95% CI)	P value
Clinical features				
Age>60 years	0.99 (0.41-1.99)	0.841		
Male sex	0.87 (0.41-2.01)	0.452		
HBV infection	0.78 (0.35-1.60)	0.414		
HCV infection	1.98 (0.32-6.56)	0.282		
BCLC stage B-C	4.18 (1.62-8.46)	<0.001	2.44 (0.95-6.22)	0.063
AFP>400 ng/ml	1.71 (0.86-2.46)	0.153		
PIVKA-II>300 mAU/mL	2.17 (1.12-4.21)	0.023	0.66 (0.26-1.68)	0.385
General macroscopic				
Tumor size > 5 cm	2.29 (0.79-6.62)	0.125		
Multiplicity	0.04 (0.00-89.84)	0.420		
Macrovascular invasion	4.65 (1.30-16.61)	0.018	5.07 (1.82-13.31)	0.001
General microscopic				
Edmondson grade III-IV	2.57 (1.90-5.13)	0.007	1.12 (0.43-2.89)	0.821
Microtrabecular	0.42 (0.20-1.01)	0.064		
Macrotrabecular	2.35 (1.16-4.93)	0.017	1.48 (0.59-3.71)	0.405
Pseudoglandular	0.99 (0.41-2.05)	0.842		
Compact	1.22 (0.62-2.02)	0.522		
Microvascular invasion	14.58 (2.69-51.86)	0.001	6.11 (1.42-26.54)	0.015

Capsule infiltration	2.25 (1.43-4.59)	0.028	1.34 (0.57-3.11)	0.502
Cirrhosis	1.36 (0.70-2.74)	0.302		
Tumoral cytological findings				
Tumoral cholestasis	0.55 (0.19-1.94)	0.378		
Clear cells	1.60 (0.71-3.10)	0.197		
Pleomorphic cells	1.82 (0.78-3.58)	0.135		
Multinucleated cells	1.40 (0.59-3.24)	0.087		
Hyaline bodies	1.14 (0.40-2.95)	0.898		
Tumoral variants				
Scirrhous	0.05 (0.00-8226.41)	0.680		
Lymphoepithelioma-like	0.05 (0.00-4206.91)	0.387		
Sarcomatoid	0.05 (0.00-1216.90)	1.000		
Steatohepatitic	1.30 (0.18-9.54)	0.795		
Macrotrabecular-massive	1.43 (0.55-3.69)	0.461		
Phenotypic markers				
VETC	2.66 (1.36-5.19)	0.004	2.84 (1.29-6.26)	0.010
Molecular phenotype[1]				
p53+	1.14 (0.56-2.20)	0.724		
β-catenin/GS+	1.04 (0.44-2.61)	0.871		
Double positive	0.05 (0.00-421.38)	0.511		
Double negative	0.98 (0.47-1.89)	0.937		

VETC, vessel encapsulating tumor clusters
[1]p53+: p53+ and βcatenin/GS-; βcatenin/GS+: p53- and βcatenin/GS+; double positive: p53+ and βcatenin/GS+; double negative: p53- and βcatenin/GS-

Table 7. Univariable and multivariable analysis on extrahepatic metastasis

Variables	Extrahepatic metastasis			
	HR (95% CI)	P value	HR (95% CI)	P value
Clinical features				
Age>60 years	0.88 (0.32-2.45)	0.810		
Male sex	0.52 (0.20-1.32)	0.166		
HBV infection	0.72 (0.24-2.17)	0.557		
HCV infection	1.66 (0.22-12.46)	0.622		
BCLC stage B-C	5.01 (2.14-9.42)	<0.001	1.65 (0.26-7.76)	0.747
AFP>400 ng/ml	1.66 (0.63-4.36)	0.307		
PIVKA-II>300 mAU/mL	2.47 (1.41-4.11)	0.001	1.09 (0.48-2.47)	0.843
General macroscopic				
Tumor size > 5 cm	3.60 (2.28-6.23)	<0.001	2.44 (1.62-4.56)	0.006
Multiplicity	2.10 (108-4.05)	0.030	2.24 (1.10-4.54)	0.026
Macrovascular invasion	7.21	<0.001	2.13 (0.65-6.95)	0.210

	(3.74-16.96)			
General microscopic				
Edmondson grade III-IV	2.28 (1.25-4.79)	0.007	0.68 (0.28-1.63)	0.384
Microtrabecular	0.77 (0.26-2.34)	0.650		
Macrotrabecular	2.40 (1.38-4.32)	0.003	1.31 (0.59-2.88)	0.509
Pseudoglandular	0.41 (0.09-1.76)	0.229		
Compact	1.73 (0.70-4.26)	0.232		
Microvascular invasion	5.96 (2.60-11.65)	<0.001	3.12 (1.33-7.56)	0.010
Capsule infiltration	2.31 (1.50-3.76)	0.012	0.76 (0.33-1.70)	0.498
Cirrhosis	0.61 (0.24-1.54)	0.293		
Tumoral cytological findings				
Tumoral cholestasis	0.04 (0.00-36.77)	0.361		
Clear cells	1.46 (0.57-3.70)	0.429		
Pleomorphic cells	2.13 (1.26-3.25)	0.007	1.27 (0.48-3.32)	0.627
Multinucleated cells	1.73 (1.11-3.23)	0.022	2.05 (0.62-6.74)	0.239
Hyaline bodies	1.06 (0.25-4.60)	0.936		
Tumoral variants				
Scirrhous	0.05 (0.00-5723.01)	0.613		
Lymphoepithelioma-like	0.83 (0.11-6.26)	0.860		
Sarcomatoid	0.05 (0.00-5064.03)	<0.001	-	-
Steatohepatitic	0.88 (0.18-6.54)	0.895		
Macrotrabecular-massive	1.58 (0.74-3.37)	0.231		
Phenotypic markers				
VETC	2.47 (1.42-4.29)	0.001	2.38 (1.21-4.64)	0.011
Molecular phenotype[1]				
p53+	2.39 (0.85-6.72)	0.099		
β-catenin/GS+	0.04 (0.00-163.57)	0.456		
Double positive	0.05 (0.00-126.58)	0.449		
Double negative	0.64 (0.23-1.80)	0.396		

VETC, vessel encapsulating tumor clusters
[1]p53+: p53+ and βcatenin/GS-; βcatenin/GS+: p53- and βcatenin/GS+; double positive: p53+ and βcatenin/GS+; double negative: p53- and βcatenin/GS-

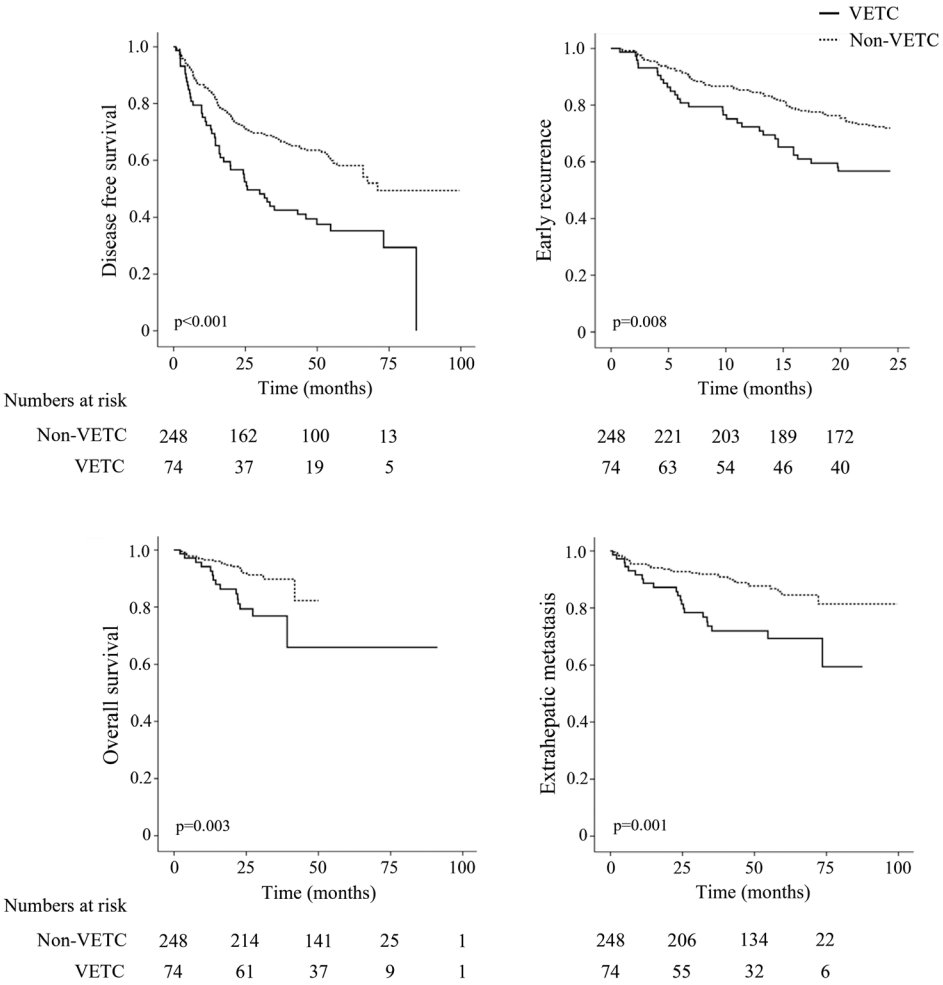

Figure 3. Kaplan-Meier curves of disease free survival (DFS), early recurrence, overall survival (OS), and extrahepatic metastasis. Vessels encapsulating tumor clusters (VETC)-hepatocellular carcinoma (HCC) showed poorer DFS, early relapse, OS, and extrahepatic metastasis than non-VETC HCC.

3. VETC is enriched in the MTM subtype HCC.

VETC was significantly enriched in the MTM subtype HCC (55.9% and 19.1%, p<0.001). The MTM subtype as seen in 10.6% (34 of 322) of HCCs and it was not associated with specific etiological factors. MTM showed a

significant correlation with clinical and pathological features of aggressiveness: advanced BCLC stage, high AFP serum levels (>400 ng/mL), macro- and microvascular invasion, Edmondson grade III-IV, and less microtrabecular pattern, capsule infiltration, pleomorphic and multinucleated cells ($p<0.05$ for all). Among the gross morphological types, MTM subtype was associated with nodular with perinodular extension subtype ($p=0.002$). Interestingly, among molecular phenotypes, MTM was significantly higher in p53+ and lower in double negative group ($p<0.05$ for all) (Table 8). MTM showed no significant difference in early recurrence, DFS, OS and extrahepatic metastasis in univariable analysis (Figure 4).

Table 8. Comparison of clinicopathological features of MTM and non-MTM-HCC

Variables	Non-MTM-HCC (n=288, n [%])	MTM-HCC (n=34, n [%])	p-value
Clinical features			
Age (> 60 years)	99 (34.3)	8 (23.5)	0.250
Male gender	233 (80.9)	26 (76.5)	0.647
Etiology			
HBV infection	236 (81.9)	29 (85.3)	0.653
HCV infection	16 (5.6)	2 (5.9)	1.000
Alcohol intake	14 (4.9)	1 (2.9)	0.718
BCLC stage B-C	21 (7.3)	7 (20.6)	0.018
Serum AFP>400 ng/ml	49 (17.0)	17 (50.0)	<0.001
Serum PIVKA-II>300 mAU/mL	82 (28.5)	12 (35.3)	0.428
Macroscopic pathological features			
Tumor size > 5 cm	57 (19.8)	7 (20.6)	1.000
Multiplicity	31 (10.8)	6 (17.6)	0.253
Macrovascular invasion	9 (3.1)	4 (11.8)	0.037
Gross morphology			
Vaguely nodular	8 (2.8)	0 (0.0)	0.608
Expanding	149 (51.7)	12 (35.3)	0.102
Nodular with perinodular extension	26 (9.0)	10 (29.4)	0.002
Multinodular confluent	90 (31.2)	10 (29.4)	0.849
Infiltrative	15 (5.2)	2 (5.9)	0.697
Microscopic pathological features			
Edmondson grade III-IV	153 (53.1)	29 (85.3)	<0.001
Architectural pattern			
Microtrabecular	261 (90.6)	21 (61.8)	<0.001

Macrotrabecular	125 (43.4)	34 (100.0)	<0.001
Pseudoglandular	108 (37.5)	7 (20.6)	0.059
Compact	95 (33.0)	10 (29.4)	0.705
Microvascular invasion	160 (55.6)	26 (76.5)	0.026
Capsule infiltration	51 (17.7)	15 (44.1)	0.001
Cirrhosis of background liver	155 (53.8)	19 (55.9)	0.857
Tumoral cytological findings			
Tumoral cholestasis	41 (14.2)	4 (11.8)	0.800
Clear cells	82 (28.5)	13 (38.2)	0.320
Pleomorphic cells	65 (22.6)	17 (50.0)	0.001
Multinucleate cells	81 (28.1)	21 (61.8)	<0.001
Sarcomatous change	2 (0.7)	0 (0.0)	1.000
Hyaline bodies	34 (11.8)	7 (20.6)	0.170
Tumoral variants			
Scirrhous	3 (1.0)	0 (0.0)	1.000
Lymphoepithelioma-like	3 (1.0)	0 (0.0)	1.000
Sarcomatoid	1 (0.3)	0 (0.0)	1.000
Steatohepatitic	5 (1.7)	2 (5.9)	0.162
Molecular phenotype[1]			
p53+	75 (26.6)	16 (51.6)	0.006
β-catenin,GS+	49 (17.4)	5 (16.1)	1.000
Double positive	8 (2.8)	0 (0.0)	1.000
Double negative	150 (52.1)	10 (29.4)	0.036
VETC phenotype	55 (19.1)	19 (55.9)	<0.001

MTM, macrotrabecular-massive subtype; VETC, vessel encapsulating tumor clusters

[1]p53+: p53+ and βcatenin/GS-; βcatenin/GS+: p53- and βcatenin/GS+; double positive: p53+ and βcatenin/GS+; double negative: p53- and βcatenin/GS-

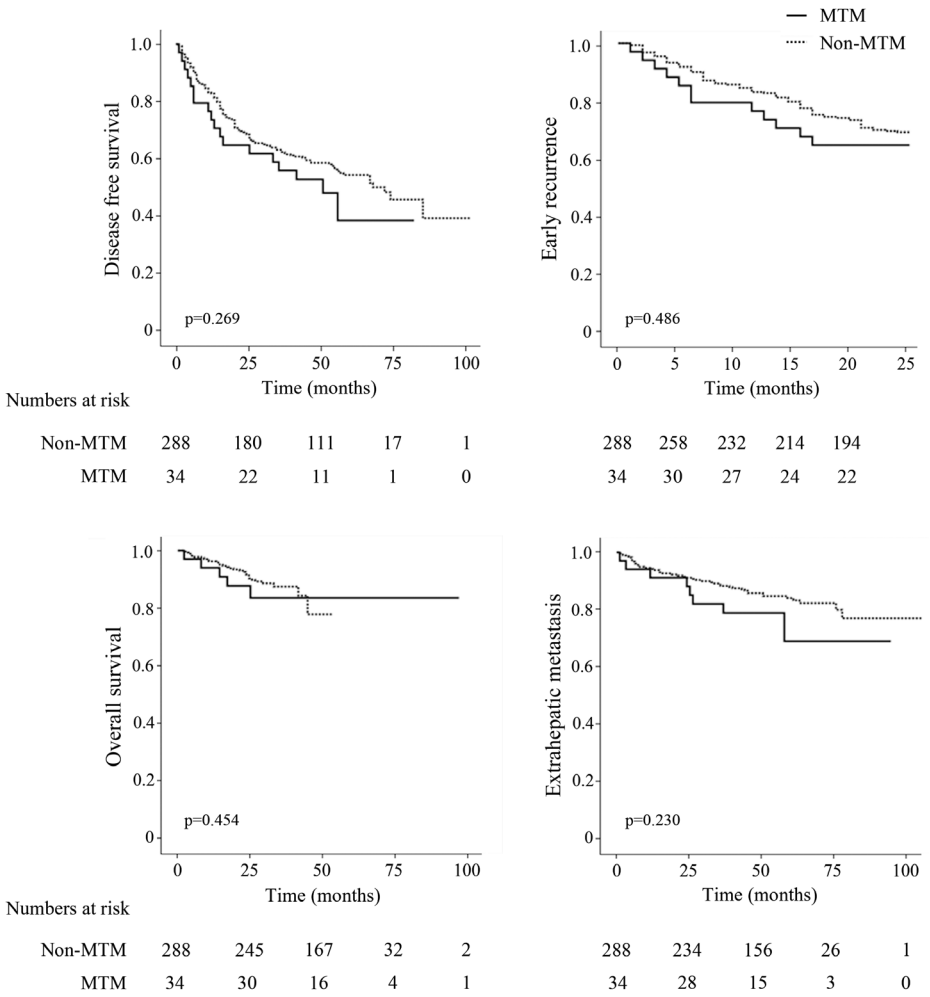

Figure 4. Kaplan-Meier curves of disease free survival (DFS), early recurrence, overall survival (OS), and extrahepatic metastasis. Macrotrabecular-massive (MTM)-hepatocellular carcinoma (HCC) showed no significant clinical impact on DFS, early relapse, OS, and extrahepatic metastasis.

4. Clinical, pathological, and phenotypical features according to molecular subgroups.

The molecular subgroups were also associated with several clinical and pathological features. p53+ HCCs accounted for 29.1% of the total cases and

were correlated with lower level of serum AFP level (<400 ng/ml), vaguely nodular gross type, pleomorphic and multinucleated cells ($p<0.05$ for all). Wnt+ HCCs were 17.3% of the cases and associated with several aggressive clinical features: older patients (>60 years), alcohol intake, and higher level of serum PIVKA-II (>300 mAU/mL, $p<0.05$ for all). Also, Wnt+ HCCs showed more tumoral cholestasis and VETC phenotype than non-Wnt+ HCCs ($p=0.017$). The molecular phenotypes did not show significant association with DFS, early recurrence, OS, and extrahepatic metastasis (Table 4-7).

Table 9. Comparison of clinicopathological features of p53+ HCC and non-p53+ HCC

Variables	Non-p53+ HCC (n=222, n [%])	p53+ HCC (n=91, n [%])	p-value
Clinical features			
Age (> 60 years)	73 (32.9)	33 (36.3)	0.600
Male gender	180 (81.1)	74 (81.3)	1.000
Etiology			
HBV infection	183 (82.4)	74 (81.3)	0.871
HCV infection	12 (5.4)	5 (5.5)	1.000
Alcohol intake	11 (5.0)	4 (4.4)	1.000
BCLC stage B-C	12 (5.4)	10 (11.0)	0.091
Serum AFP > 400 ng/ml	54 (24.3)	10 (11.0)	0.008
Serum PIVKA-II > 300 mAU/mL	66 (29.7)	25 (27.5)	0.784
Macroscopic pathological features			
Tumor size > 5 cm	46 (20.7)	14 (15.4)	0.343
Multiplicity	23 (10.4)	14 (15.4)	0.253
Macrovascular invasion	7 (3.2)	3 (3.3)	1.000
Gross morphology			
Vaguely nodular	3 (1.4)	5 (5.5)	0.049
Expanding	116 (52.3)	42 (46.2)	0.384
Nodular with perinodular extension	25 (11.3)	10 (11.0)	1.000
Multinodular confluent	67 (30.2)	30 (33.0)	0.687
Infiltrative	11 (5.0)	4 (4.4)	1.000
Microscopic pathological features			
Edmondson grade III-IV	121 (54.5)	52 (57.1)	0.708
Architectural pattern			
Microtrabecular	195 (87.8)	78 (85.7)	0.709
Macrotrabecular	109 (49.1)	44 (48.4)	1.000
Pseudoglandular	81 (36.5)	32 (35.2)	0.897
Compact	75 (33.8)	25 (27.5)	0.289

Microvascular invasion	130 (58.6)	48 (52.7)	0.380
Capsule infiltration	41 (18.5)	16 (17.6)	0.874
Cirrhosis of background liver	126 (56.8)	44 (48.4)	0.211
Tumoral cytological findings			
Tumoral cholestasis	37 (16.7)	8 (8.8)	0.078
Clear cells	60 (27.0)	33 (36.3)	0.134
Pleomorphic cells	43 (19.4)	30 (33.0)	0.012
Multinucleate cells	58 (26.1)	36 (39.6)	0.021
Sarcomatous change	0 (0.0)	1 (1.1)	0.291
Hyaline bodies	28 (12.6)	12 (13.2)	1.000
Tumoral variants			
Scirrhous	3 (1.4)	0 (0.0)	0.559
Lymphoepithelioma-like	3 (1.4)	0 (0.0)	0.559
Sarcomatoid	0 (0.0)	0 (0.0)	1.000
Steatohepatitic	3 (1.4)	4 (4.4)	0.200
VETC phenotype	53 (23.9)	16 (17.6)	0.235

Table 10. Comparison of clinicopathological features of Wnt+ HCC and non-Wnt+ HCC

Variables	Non-Wnt+ HCC (n=259, n [%])	Wnt+ HCC (n=54, n [%])	p-value
Clinical features			
Age (> 60 years)	80 (30.9)	26 (48.1)	0.018
Male gender	208 (80.3)	46 (85.2)	0.451
Etiology			
HBV infection	216 (83.4)	41 (75.9)	0.240
HCV infection	14 (5.4)	3 (5.6)	1.000
Alcohol intake	9 (3.5)	6 (11.1)	0.029
BCLC stage B-C	17 (6.6)	5 (9.3)	0.556
Serum AFP > 400 ng/ml	56 (21.6)	8 (14.8)	0.276
Serum PIVKA-II > 300 mAU/mL	69 (26.6)	22 (40.7)	0.048
Macroscopic pathological features			
Tumor size > 5 cm	46 (17.8)	14 (25.9)	0.184
Multiplicity	31 (12.0)	6 (11.1)	1.000
Macrovascular invasion	9 (3.5)	1 (1.9)	1.000
Gross morphology			
Vaguely nodular	8 (3.1)	0 (0.0)	0.359
Expanding	124 (47.9)	34 (63.0)	0.052
Nodular with perinodular extension	26 (10.0)	9 (16.7)	0.233
Multinodular confluent	87 (33.6)	10 (18.5)	0.035
Infiltrative	14 (5.4)	1 (1.9)	0.330
Microscopic pathological features			
Edmondson grade III-IV	144 (55.6)	29 (53.7)	0.881
Architectural pattern			
Microtrabecular	224 (86.5)	49 (90.7)	0.504

Macrotrabecular	120 (46.3)	33 (61.1)	0.053
Pseudoglandular	89 (34.4)	24 (44.4)	0.165
Compact	81 (31.3)	19 (35.2)	0.631
Microvascular invasion	142 (54.8)	36 (66.7)	0.131
Capsule infiltration	46 (17.8)	11 (20.4)	0.699
Cirrhosis of background liver	140 (54.1)	30 (55.6)	0.881
Tumoral cytological findings			
Tumoral cholestasis	31 (12.0)	14 (25.9)	0.017
Clear cells	81 (31.3)	12 (22.2)	0.196
Pleomorphic cells	63 (24.3)	10 (18.5)	0.385
Multinucleate cells	80 (30.9)	14 (25.9)	0.517
Sarcomatous change	1 (0.4)	0 (0.0)	1.000
Hyaline bodies	33 (12.7)	7 (13.0)	1.000
Tumoral variants			
Scirrhous	3 (1.2)	0 (0.0)	0.644
Lymphoepithelioma-like	3 (1.2)	0 (0.0)	0.644
Sarcomatoid	0 (0.0)	0 (0.0)	1.000
Steatohepatitic	7 (2.7)	0 (0.0)	0.609
VETC phenotype	43 (16.6)	26 (48.1)	<0.001

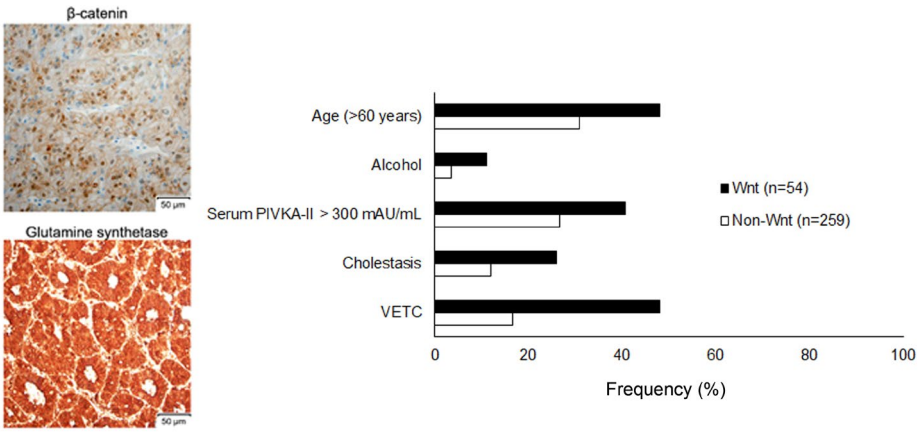

Figure 5. Clinicopathologic features associated with Wnt+ HCCs

5. The TME of VETC-HCCs

To evaluate the TME of VETC-HCCs, we analyzed various aspects of TME: 1) EMT: expression of Zeb1, Snail, Ezrin, S100A4 and loss of E-cadherin; 2) Fibrous tumor stroma: histological evaluation and expression of cancer-associated fibroblast (CAF, αSMA and FAP); 3) Stemness: K19; 4) Hypoxia: CAIX; 5) Tumor immunity: immune cell infiltration, macrophage

infiltration (CD163) and PD-L1.

As a result, VETC-HCCs demonstrated several distinct features related to TME as follows: EMT-low, scarce fibrous stroma, more CAIX expression, less immune cell infiltration, and less PD-L1 expression by immune cells, compared to non-VETC-HCCs ($p<0.05$ for all, Table 11). In contrast, non-VETC-HCCs exhibited EMT-high, abundant fibrous stroma, high immune cell infiltration, more PD-L1 expression by immune cells ($p<0.05$ for all).

Table 11. Comparison of TME-related features of VETC-HCCs and non-VETC-HCCs

Variables	VETC-HCCs (n=74, n [%])	Non-VETC-HCCs (n=248, n [%])	p-value
EMT-high[1]	1 (1.4)	52 (21.0)	<0.001
Fibrous tumor stroma[2]	10 (13.5)	117 (47.2)	<0.001
Cancer-associated fibroblast			
αSMA	8 (10.8)	73 (29.4)	0.001
FAP	5 (6.8)	54 (21.8)	0.003
K19	6 (8.1)	38 (15.3)	0.126
CAIX	14 (18.9)	16 (6.5)	0.002
High immune cell infiltration[3]	4 (5.4)	104 (41.9)	<0.001
CD163+ macrophage	24 (32.4)	101 (40.7)	0.223
PD-L1 (tumor)	15 (20.3)	73 (29.4)	0.138
PD-L1 (immune cell)	6 (8.1)	58 (23.4)	0.004

TME, tumor microenvironment; VETC, vessel encapsulating tumor clusters; HCC, hepatocellular carcinoma; EMT, epithelial-mesenchymal transition
[1]EMT-high denotes positivity in more than 3 out of 5 EMT-related markers
[2]Fibrous tumor stroma denotes fibrous band intervening tumor nests ≥20% of tumor surface area
[3]High immune cell infiltration was defined as mononuclear cells ≥10% of tumor surface area or density of tertiary lymphoid stroma ≥ 5 foci.

We observed that the TME of non-VETC-HCCs were of more heterogeneity, whereas the TME of VETC-HCCs was rather homogenous. In other words, non-VETC-HCCs showed varying degree of fibrous stroma and associated inflammatory cell infiltration, whereas VETC-HCCs lacked fibrous

stroma and inflammatory cell infiltration. Therefore, non-VETC-HCCs were further divided into those with and without fibrous tumor stroma (FTS). Consequently, HCCs were classified into 3 groups; VETC-HCCs (n=74, 23.0%); non-VETC-HCCs with FTS (n=117, 36.3%); non-VETC-HCCs without FTS (n=131, 40.7%, Figure 3).

Non-VETC-HCCs with FTS showed several distinct features of TME, compared to other groups: EMT-high (32.5%), K19 expression (21.4%), high immune cell infiltration (64.1%), CD163+ macrophages infiltration (50.4%), PD-L1 expression by tumor (41.9%), and immune cells (31.6%, $p<0.05$ for all). Non-VETC-HCCs without FTS showed a middle level of the EMT signature and immune cell infiltration among the three groups and similar level of K19 expression as that of VETC-HCCs. On the other hand, VETC-HCCs demonstrated significantly enhanced CAIX expression (18.9%) than other groups ($p<0.05$ for all). Interestingly, VETC-HCCs and non-VETC-HCCs without FTS have no fibrous stroma in common, non-VETC-HCCs without FTS showed more EMT-high, less CAIX expression, high immune cell infiltration than VETC-HCCs.

According to molecular phenotype, VETC-HCCs were significantly associated with Wnt+ (37.7%, $p<0.05$ for all) and non-VETC-HCCs with FTS with double negative (68.1%, $p<0.05$ for all). Non-VETC-HCCs without FTS were correlated with p53+ (36.6%) than non-VETC-HCCs with FTS (23.9%, $p=0.037$).

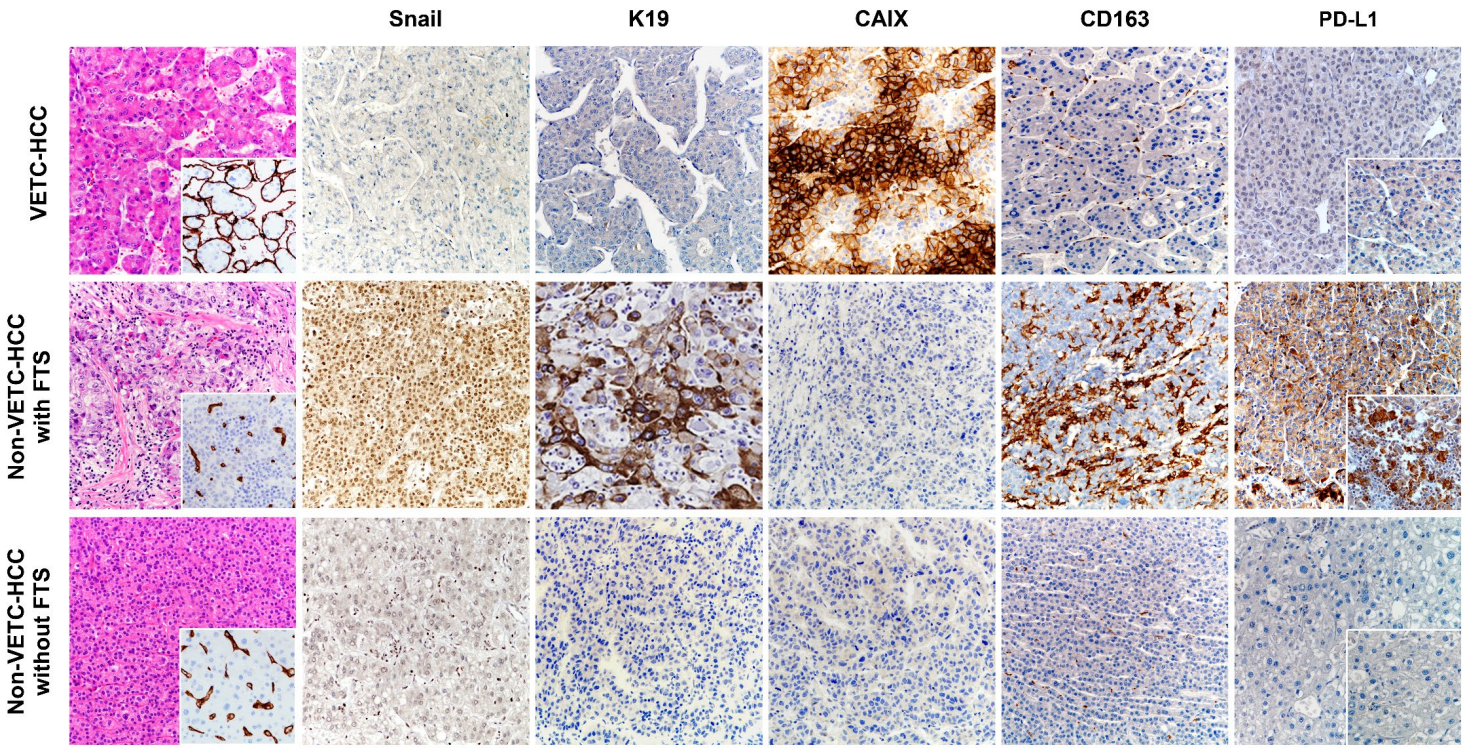

Figure 6. Representative images of each group. H&E (inset: CD34), epithelial-mesenchymal transition (Snail), stemness (K19), hypoxia (CAIX), tumor-associated macrophage (CD163), and PD-L1 expression by tumor cells (inset: PD-L1 expression by immune cells) (200X magnification).

Table 12. Comparison of TME-related features in each group.

Variables	VETC-HCC, n (%) (group 1, n=74)	Non-VETC-HCC, n (%)		p-value			
		FTS (group 2, n=117)	No FTS (group 3, n=131)	Group 1 and 2	Group 1 and 3	Group 2 and 3	Group 1 and 2 and 3
EMT-high[1]	1 (1.4)	38 (32.5)	14 (10.7)	<0.001	0.012	<0.001	<0.001
Fibrous tumor stroma[2]	10 (13.5)	117 (100.0)	0 (0.0)	<0.001	<0.001	<0.001	<0.001
Cancer-associated fibroblast							
αSMA	8 (10.8)	63 (53.8)	10 (7.6)	<0.001	0.451	<0.001	<0.001
FAP	5 (6.8)	51 (43.6)	3 (2.3)	<0.001	0.140	<0.001	<0.001
K19	6 (8.1)	25 (21.4)	13 (9.9)	0.016	0.804	0.014	0.009
CAIX	14 (18.9)	10 (8.5)	6 (4.6)	0.044	0.001	0.300	0.003
High immune cell infiltration[3]	4 (5.4)	75 (64.1)	29 (22.1)	<0.001	0.003	<0.001	<0.001
CD163+ macrophage	24 (32.4)	59 (50.4)	42 (32.1)	0.017	1.000	0.004	0.005
PD-L1 (tumor)	15 (20.3)	49 (41.9)	24 (18.3)	0.003	0.853	<0.001	<0.001
PD-L1 (immune cell)	6 (8.1)	37 (31.6)	21 (16.0)	<0.001	0.134	0.004	<0.001

TME, tumor microenvironment; VETC, vessel encapsulating tumor clusters; HCC, hepatocellular carcinoma; FTS, fibrous tumor stroma; EMT, epithelial-mesenchymal transition; TAM, tumor-associated macrophage

[1]EMT-high denotes positivity in more than 3 out of 5 EMT-related markers

[2]Fibrous tumor stroma denotes fibrous band intervening tumor nests ≥20% of tumor surface area

[3]High immune cell infiltration was defined as mononuclear cells ≥10% of tumor surface area or density of tertiary lymphoid stroma ≥ 5 foci.

6. Survival analysis of each group

On survival analysis of three groups, patients with VETC-HCCs revealed poorer prognosis, compared to patients with non-VETC-HCCs without FTS, in all prognostic parameters ($p<0.05$ for all). The clinical impact of VETC-HCCs was a bit reduced when compared to non-VETC-HCCs with FTS. Still, it showed significantly shorter DFS ($p=0.009$) than non-VETC-HCCs with FTS and a tendency toward more extrahepatic metastasis ($p=0.060$). On comparison among patients with non-VETC-HCCs, patients with non-VETC-HCCs with FTS demonstrated shorter OS ($p=0.005$) and an approaching significance to extrahepatic metastasis ($p=0.070$), than patients in non-VETC-HCCs without FTS.

Overall, the patients with VETC-HCCs had the worst outcome, patients with non-VETC-HCCs without FTS had the best prognosis, patients with non-VETC-HCCs with FTS were in the middle. ($p<0.05$ for all, figure 7).

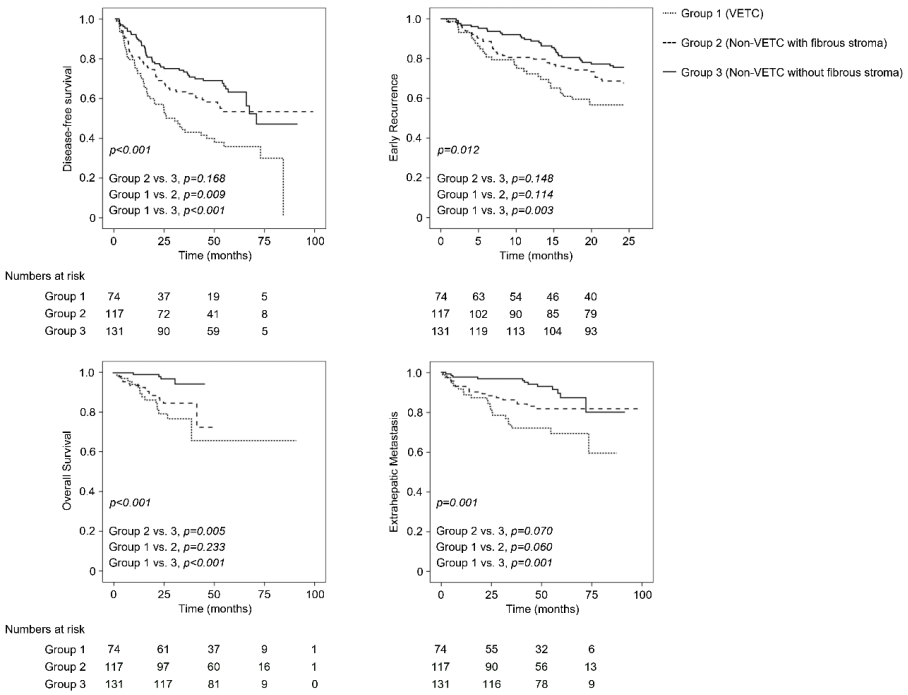

Figure 7. Kaplan-Meier curves of DFS, early recurrence, OS, and extrahepatic metastasis.

7. Comparison of intrahepatic primary HCCs and extrahepatic metastatic HCCs

We collected 130 cases of extrahepatic metastasis of HCCs (cohort 2, Table 13): 116 cases were from the first metastatic lesion, and 14 cases were from the second or more. The most common metastastic site was lung (n=64, 49.2%), followed by lymph node (n=19, 14.6%), bone (n=18, 13.8%), brain (n=17, 13.1%), adrenal gland (n=11, 8.5%), and spleen (n=1, 0.8%). The median interval time between initial diagnosis of primary tumor and detection of metastatic tumor was 24 months. Seven patients had synchronous extrahepatic metastasis with intrahepatic primary HCCs (lymph node: 2 cases; lung: 2 cases; adrenal gland: 2 cases, and bone: 1 case).

Table 13. Baseline characteristics of the extrahepatic metastatic HCCs (cohort 2, n=130).

Variables	Mean ± SD or n (%)
Age (years)	55.6 ± 10.3
Male sex	101 (77.7)
Etiology (HBV/HCV/alcohol/others)	112 (86.2)/7 (5.4)/5 (3.8)/6 (4.6)
Serum AFP (ng/mL)	2220.2 ± 10099.1
Serum PIVKA-II (mAU/mL)	418.4 ± 646.7
Interval time from the first diagnosis (months)	24.1 ± 19.6
Metastatic site	
Lung	64 (49.2)
Lymph node	19 (14.6)
Bone	18 (13.8)
Brain	17 (13.1)
Adrenal gland	11 (8.5)
Spleen	1 (0.8)

A. Comparison of general pathological features and TME-related features of intrahepatic primary HCCs and extrahepatic metastatic HCCs.

We analyzed several pathological features including tumor differentiation; architectural pattern (micro/macrotrabecular, pseudoglandular, and compact); sarcomatous change and MTM subtype (Table 14).

Tumors with poor differentiation (Edmondson-steiner grade III-IV) were noted 56.5% of primary tumors and 47.7% of metastatic tumors (p=0.096). For architectural patterns, primary intrahepatic HCCs demonstrated higher incidence of microtrabecular (87.6%), pseudoglandular (35.7%), and compact (32.6%) growth, compared to 36.9%, 16.9%, and 22.3% in extrahepatic metastatic HCCs ($p<0.05$ for all). Macrotrabecular pattern (40.8%) was the most common architectural pattern in extrahepatic metastatic HCCs, and MTM subtype was nearly twice as compared to the primary intrahepatic

HCCs (20.8% and 10.6%, p=0.006). HCCs with sarcomatous change were rarely observed in both groups, and there was no significant difference (0.6% and 1.5%, p=0.326). The VETC phenotype was consistently found in both groups (23.0% and 21.4%, p=0.797).

Table 14. Comparison of general pathological and TME-related features between primary and extrahepatic metastatic HCC

Variables	Primary intrahepatic HCCs, %	Extrahepatic metastasis of HCCs, %	p-value
General pathological features			
Edmondson grade III-IV	56.5 (182/322)	47.7 (62/130)	0.096
Architectural pattern			
Microtrabecular	87.6 (282/322)	36.9 (48/130)	<0.001
Macrotrabecular	49.4 (159/322)	40.8 (53/130)	0.118
Pseudoglandular	35.7 (115/322)	16.9 (22/130)	<0.001
Compact	32.6 (105/322)	22.3 (29/130)	0.031
Sarcomatous change	0.6 (2/322)	1.5 (2/130)	0.326
Macrotrabecular-massive subtype	10.6 (34/322)	20.8 (27/130)	0.006
Tumor vessel: VETC	23.0 (74/322)	19.7 (23/117)	0.516
Tumor microenvironmental features			
EMT-high[1]	16.5 (53/322)	26.1 (31/119)	0.029
Fibrous tumor stroma[2]	39.4 (127/322)	14.6 (19/130)	<0.001
Cancer-associated fibroblast			
αSMA	20.8 (67/322)	24.4 (29/119)	0.437
FAP	25.2 (79/313)	14.3 (17/119)	0.014
CAIX	9.3 (30/322)	24.3 (28/115)	<0.001
K19	13.7 (44/322)	27.7 (36/130)	0.001
High immune cell infiltration[3]	33.5 (108/322)	20.0 (26/130)	0.004
CD163+ macrophage	38.6 (119/308)	27.7 (33/119)	0.042
PD-L1 (Tumor)	27.3 (88/322)	19.3 (23/119)	0.108
PD-L1 (Immune cell)	19.9 (64/322)	21.0 (25/119)	0.894

TME, tumor microenvironment; HCC, hepatocellular carcinoma; VETC, vessels encapsulating tumor cluster; EMT, epithelial-mesenchymal transition; TAM, tumor-associated macrophage
[1]EMT-high denotes positivity in more than 3 out of 5 EMT-related markers
[2]Fibrous tumor stroma denotes fibrous band intervening tumor nests ≥20% of tumor area
[3]High immune cell infiltration was defined as mononuclear cells ≥10% of surface area or density of tertiary lymphoid stroma ≥ 5 foci.

In terms of TME-related features, extrahepatic metastatic lesions showed significantly EMT-high, CAIX and K19 expression ($p<0.05$ for all), whereas intrahepatic HCCs comprised of more abundant fibrous stroma, rich immune cell infiltration, and more CD163+ macrophages infiltration than metastatic lesions ($p<0.05$ for all). PD-L1 expression in either tumor cells or immune cells and cancer-associated fibroblast (FAP and αSMA) expression was not significantly different in the both groups.

As EMT has been considered as one of essential pathways for extrahepatic metastasis, we further divided the extrahepatic metastatic HCCs into two groups according to EMT signature: EMT-low group (n=88, 74.0%) and EMT-high group (n=31, 26.1%) (Table 15). MTM subtype was constantly observed in both groups (22.7% and 22.6%, p=1.000), whereas VETC was significantly associated with EMT-low group (25.9% and 6.5%, p=0.036). EMT-high group was correlated with abundant fibrous stroma, K19 expression, high immune cell infiltration, and high expression of PD-L1 by tumor and immune cells ($p<0.05$ for all). On the other hand, EMT-low group exhibited less fibrous stroma and less K19 expression, less immune cell infiltration and low expression of PD-L1 by tumor and immune cells ($p<0.05$ for all).

Table 15. Comparison of extrahepatic metastatic HCCs according to EMT signature.

Variables	EMT-low group, %	EMT-high group, %	p-value
Pathological features			
Macrotrabecular-massive	22.7 (20/88)	22.6 (7/31)	1.000
Tumor vessel: VETC	25.9 (22/85)	6.5 (2/31)	0.036
Tumor microenvironmental features			
Fibrous tumor stroma[1]			
Cancer-associated fibroblast			
αSMA	6.8 (6/88)	51.6 (16/31)	<0.001
FAP	4.5 (4/88)	35.5 (11/31)	<0.001
CAIX	25.9 (22/85)	20.7 (6/29)	0.628
K19	18.2 (16/88)	58.1 (18/31)	<0.001
High immune cell infiltration[2]	12.5 (11/88)	48.4 (15/31)	<0.001
CD163	22.7 (20/88)	41.9 (13/31)	0.061
PD-L1 (Tumor)	11.4 (10/88)	41.9 (13/31)	0.001
PD-L1 (Immune cell)	14.8 (13/88)	38.7 (12/31)	0.009

HCC, hepatocellular carcinoma; EMT, epithelial-mesenchymal transition; VETC, vessels encapsulating tumor cluster; TAM, tumor-associated macrophage

[1]Fibrous tumor stroma denotes fibrous band intervening tumor nests ≥20% of tumor area

[2]High immune cell infiltration was defined as mononuclear cells ≥10% of surface area or density of tertiary lymphoid stroma ≥ 5 foci.

B. Histological and immunohistochemical results among various extrahepatic metastatic sites.

MTM subtype and VETC were most commonly observed in lung metastasis (32.8% for both than other organs (adjusted p-value<0.01 for both) (Table 16 and Figure 8). MTM subtype and VETC were not found in any case of 19 lymph node metastasis. The metastatic lesions in lymph node showed noticeable EMT-high signature (61.1%), abundant fibrous stroma (52.6%), expression of CAF (αSMA, 50.0%; FAP, 44.4%), K19 expression (57.9%),

immune cell infiltration (63.2%), TAM infiltration (61.1%), and PD-L1 expression by tumor and immune cells (44.4% for both), compared to other metastatic organs (adjusted p-value<0.01 for all). In contrast, any cases of brain metastasis exhibited prominent immune cell infiltration nor fibrous stroma.

The frequency of VETC phenotype was consistent in lung, bone, and adrenal gland metastasis (32.8%, 25.0%, and 22.2%, respectively), whereas any of metastatic lesions at lymph node or brain were not of VETC phenotype. For markers of CAF, any lesions in brain metastasis did not showed FAP expression. CAIX expression was consistently observed among different metastatic sites (p=0.256). K19 expression was the most frequent in the lymph node metastasis (57.9%, adjusted p-value<0.008), followed by the brain metastasis (41.2%).

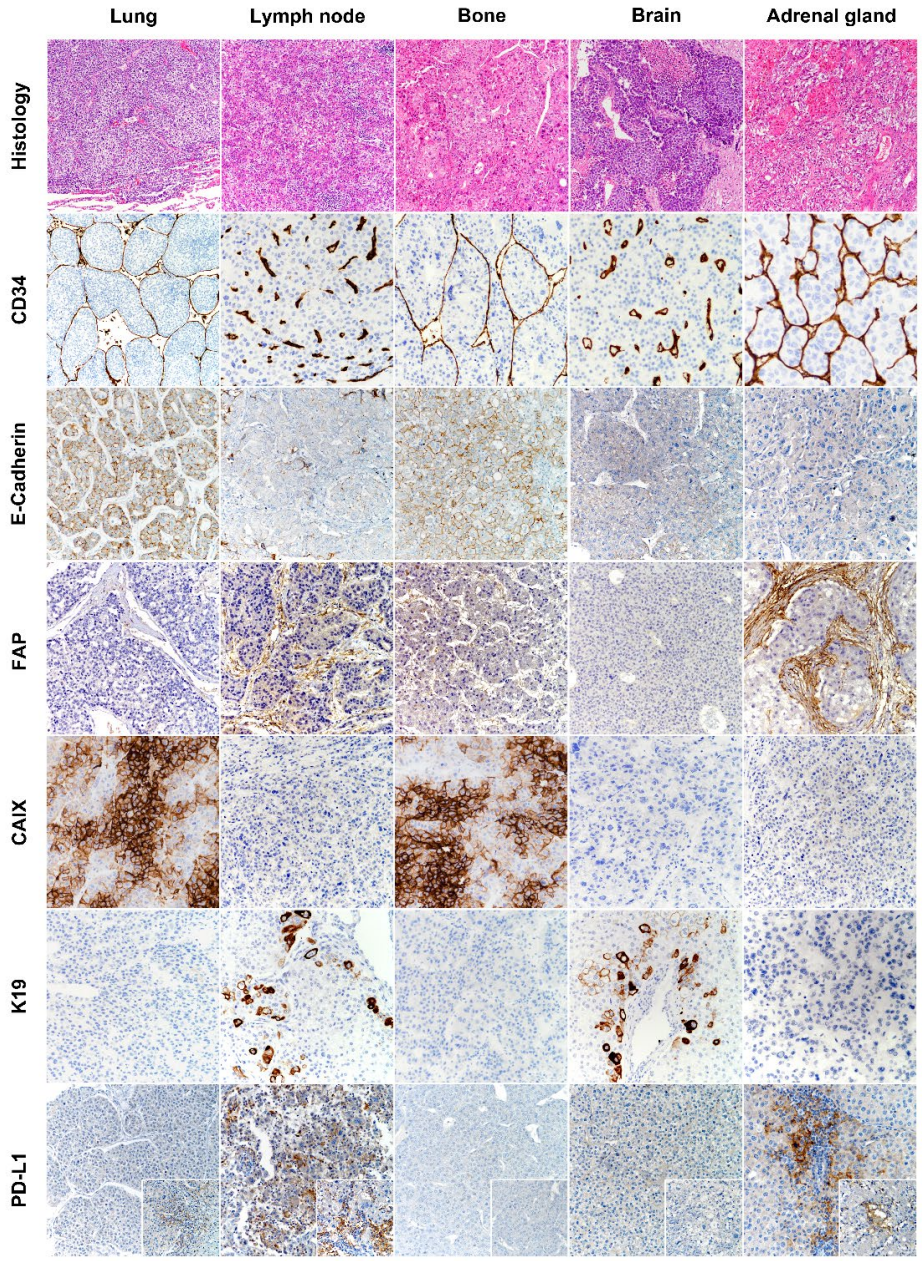

Figure 8. Representative images of extrahepatic metastasis of HCCs at various metastatic sites.

Table 16. Comparison of extrahepatic metastatic HCCs among different metastatic sites.

Variables	Lung, %	Lymph node, %	Bone, %	Brain, %	Adrenal gland, %	Total, %	p-value
Edmondson grade III-IV	46.9 (30/64)	63.2 (12/19)	44.4 (8/18)	52.9 (9/17)	27.3 (3/11)	47.7 (62/130)	0.436
Architectural pattern							
Microtrabecular	25.0 (16/64)	21.1 (4/19)	22.2 (4/18)	11.8 (2/18)	41.7 (5/12)	23.8 (31/130)	0.468
Macrotrabecular	46.9 (30/64)	26.3 (5/19)	38.9 (7/18)	47.1 (8/17)	25.0 (3/12)	40.8 (53/130)	0.403
Pseudoglandular	10.9 (7/64)	26.3 (5/19)	22.2 (4/18)	11.8 (2/17)	33.3 (4/12)	16.9 (22/130)	0.156
Compact	12.5 (8/64)	36.8 (4/19)	16.7 (3/18)	11.8 (2/17)	8.3 (1/12)	16.2 (21/130)	0.161
MTM subtype	32.8 (21/64)*	0.0 (0/19)	5.6 (1/18)	23.5 (4/17)	9.1 (1/11)	20.9 (27/129)	0.004
VETC	32.8 (19/58)*	0.0 (0/18)	25.0 (4/16)	0.0 (0/16)	22.2 (2/9)	21.4 (25/117)	0.002
EMT-high[1]	18.3 (11/60)	61.1 (11/18)*	6.2 (1/16)	31.2 (5/16)	33.3 (3/9)	26.1 (31/119)	0.002
Fibrous tumor stroma[2]	9.4 (6/64)	52.6 (10/19)*	5.6 (1/18)	0.0 (0/17)	18.2 (2/11)	14.7 (19/129)	<0.001
Cancer-associated fibroblast							
αSMA	15.0 (9/60)	50.0 (9/18)*	6.2 (1/16)	6.2 (1/16)	22.2 (2/9)	18.5 (22/119)	0.007
FAP	6.7 (4/60)	44.4 (8/18)*	6.2 (1/16)	0.0 (0/16)	22.2 (2/9)	12.6 (15/119)	0.001
CAIX	29.8 (17/57)	11.8 (2/17)	37.5 (6/16)	12.5 (2/16)	12.5 (1/8)	24.6 (28/114)	0.256
K19							
Immune cell infiltration[3]	14.1 (9/64)	63.2 (12/19)*	11.1 (2/18)	5.9 (1/17)	18.2 (2/11)	20.0 (26/129)	<0.001
CD163	16.7 (10/60)*	61.1 (11/18)*	25.0 (4/16)	31.2 (5/16)	33.3 (3/9)	27.7 (33/119)	0.008
PD-L1 (Tumor)	13.3 (8/60)	44.4 (8/18)*	18.8 (3/16)	12.5 (2/16)	22.2 (2/9)	19.3 (23/119)	0.071
PD-L1 (Immune cell)	21.7 (13/60)	44.4 (8/18)*	12.5 (2/16)	0.0 (0/16)	22.2 (2/9)	21.0 (25/119)	0.021

HCC, hepatocellular carcinoma; VETC, vessels encapsulating tumor cluster; MTM, macrotrabecular-massive; EMT, epithelial-mesenchymal transition

[1]EMT-high denotes positivity in more than 3 out of 5 EMT-related markers; [2]Fibrous tumor stroma denotes fibrous band intervening tumor nests ≥20% of tumor surface area; [3]High immune cell infiltration was defined as mononuclear cells ≥10% of tumor surface area or density of tertiary lymphoid stroma ≥ 5 foci. * Adjusted p-value < 0.01

C. Comparison of TME-related features in intrahepatic primary HCCs and their corresponding extrahepatic metastatic HCCs.

The general pathological features and TME-related features were evaluated in the intrahepatic primary HCCs and their corresponding extrahepatic metastatic HCCs (n=32) For general pathological features, about half of the tumors that initially exhibited Edmondson grade III-IV remained the same (15/25, 60.0%) and vice versa (3/7, 42.9%). Six tumors that were once MTM subtype originally, all maintained MTM subtype after metastasis. Of the 26 cases that were not of MTM subtype, 4 cases turned into MTM subtype in their metastatic sites. Of the 14 cases that were initially VETC type, only 4 cases remained VETC type and the other cases converted into non-VETC phenotype after metastasis. On the other hand, the majority of the cases that were of non-VETC phenotype, remained non-VETC phenotype after metastasis (15/18, 83.3%).

For EMT signature, most of the cases were originally EMT-low (29/32, 90.6%), most of which remained EMT-low (24/29, 82.8%), and all three cases that were originally EMT-high remained unchanged. Eight cases out of twelve cases that had apparent fibrous stroma in initial sites, revealed scant fibrous stroma in their metastatic lesions, and only three cases out of twenty cases that lacked fibrous stroma showed abundant fibrous stroma in their metastatic sites. A hypoxia-related marker (CAIX) was positive in 8 cases at primary site, but only 1 case retained positivity after metastasis, and 91.7% (22/24) of the cases that were negative for CAIX at primary site showed still negativity after metastasis. Two out of five cases that expressed stemness-related marker (K19) lost their immunoreactivity after metastasis, while most of tumors that did not expressed K19 at primary site did not showed positivity for K19 after metastasis (20/27, 74.1%).

Six of the nine primary tumors with rich immune cell infiltration, turned into tumors with less immune cell infiltration in metastatic sites, but only five

out of twenty-three cases (21.7%) of poor immune cell infiltration changed to immune-rich tumors in metastatic sites. About half of the tumors that exhibited abundant CD163+ TAM infiltration remained the same after metastasis (7/13, 53.8%), and most of tumor that originally lacked CD163+ TAM had little CD163+ macrophages after metastasis (17/19, 89.5%). PD-L1 expression by tumor cells was observed in 6 cases at primary site, but most of the cases (5/6, 83.3%) converted into negativity after metastasis. When primary tumors did not express PD-L1 by tumor cells, they generally tended to conserve negativity after metastasis (20/26, 76.9%). The trend of the PD-L1 expression by immune cells was similar to that of tumor cells. Nine cases exhibited PD-L1 expression in immune cells at primary site, but six cases changed to negativity at metastatic sites, while 16 out of 23 cases (69.6%) that were initially negative remained negativity after metastasis.

Overall, general pathological features and TME-related features were preserved after extrahepatic metastasis (McNemar's test, $p>0.05$ for all).

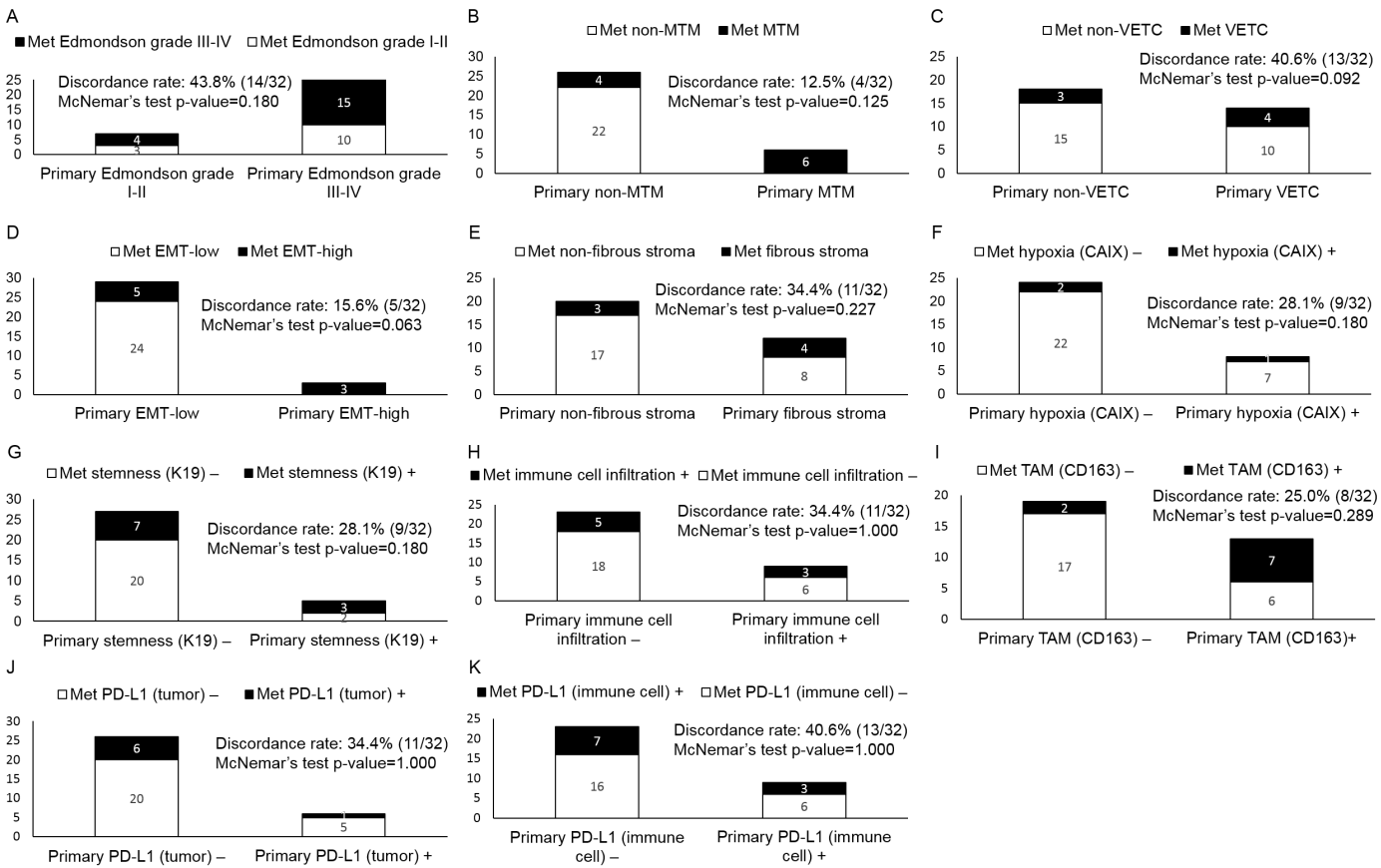

Figure 9. Comparison of various phenotypic features in matched pairs of primary and metastatic HCCs (n=32). Phenotypic difference of general pathological features (A-C), EMT and related features (D-G), and tumor immunity-related features (H-K).

IV. DISCUSSION

This study aimed to evaluate the robustness of the impact on survival and tumor environmental features of a vascularization pattern of HCC named VETC. VETC-HCCs accounted for 23.0%, regardless of etiology, a proportion of enough size to capture a consistent and clinically significant fraction of HCC. We provided a morphological tool that is easily incorporable into clinical practice with a cutoff value for VETC HCC of 55% (i.e., most of the tumor area). This cutoff revealed to be a robust prognostic parameter that discriminates aggressive HCCs with a significant impact on OS, extrahepatic metastasis and early recurrence. In addition, there was a good correlation of VETC occurrence between TMA and whole section suggested that this feature could be reliably detected in small tissue samples as in core needle biopsies. Indeed, one of the main limitations of HCC biopsy is the poor performance in the detection of microvascular invasion, an adverse prognostic feature that was well correlated with the VETC in our series. Previously, Fang et al. reported 39% VETC HCC, but in that series the authors did not use the more selective 55% cutoff value for VETC; moreover, 75% of HCCs were greater than 5 cm (versus 19.9% in the present study), suggesting that this specific vascular pattern could be related to the tumor progression[24].

Concerning molecular features, Wnt/β-catenin deregulated HCCs were 17.3% (54/313), and 48.1% (26/54) of these showed the VETC phenotype, a greater proportion compared with the Wnt/β-catenin-unrelated group (16.6%, 43/259). Actually, in the clinically robust molecular HCC classification[6], the S1 subclass—with an aberrant activation of the canonical Wnt/β-catenin pathway (by transforming growth factor β rather than by β-catenin mutations)—was characterized by a greater risk of earlier recurrence and more vascular invasion, two features in keeping with the profile of our VETC HCC. It has been also shown that the Wnt/β-catenin pathway contributes to angiogenesis by regulating the expression of angiogenic factors[32]. We are therefore tempted to speculate that VETC enrichment might have occurred in a HCC subpopulation with Wnt/β-catenin deregulation not necessarily related

to gene mutations.

Interestingly, TME of VETC showed EMT-low, scarce fibrous stroma, more CAIX expression, less immune cell infiltration, and less PD-L1 expression by immune cells, compared to non-VETC-HCCs. Recently, the immune class of HCC has been widely investigated and integrative analysis of molecular-immunologic analysis has been emerged[11-13,33]. In particular, Wnt/β-catenin pathway characterize the immune-exclusion class (cold tumor) and might represent the biomarkers predicting resistance to immunotherapy[13]. This suggest that VETC-HCCs may show primary resistance to PD-L1 inhibitors and, in turn, non-VETC-HCCs which seem to overlap with immune class (hot tumor) may benefit from PD-L1 inhibitors. Moreover, in advanced HCC, VETC has been recently suggested to act as a predictor of sorafenib benefit[25]. In other words, characterization and recognition of the TME and VETC phenotype may help customize treatment of HCC. Large-scale research of this issue is needed for personalized treatment of HCC in the future.

Interestingly, VETC-HCC was significantly enriched in MTM-HCC (55.9%, 19/34) as compared with non-MTM-HCC (19.1%, 55/288) and VETC-HCCs revealed higher expression of CAIX compared to non-VETC-HCCs. The angiogenesis activation has been considered as a hallmark biological feature of MTM-HCC[29]. Moreover, it has been reported that genes related to hypoxia (CAIX) and hypoxia-induced neoangiogenesis (ESM1) are significantly upregulated in MTM-HCCs[34]. In that VETC-HCCs and MTM-HCCs are considerably overlapping and both express CAIX in common, it might be suggested that the both phenotypes might share the similar TME. Further researches are required to investigate if MTM-HCC and VETC-HCC may be sensitive to anti-angiogenesis drugs. Noticeably, inhibitors of Ang2 and VEGFA have been reported to strongly suppress neoangiogenesis and induce tumor necrosis in various preclinical models of human cancers[35-37].

The extrahepatic metastasis of HCC is still regarded as a terminal event and various elements affecting extrahepatic metastasis of HCCs have been

investigated. It has been reported that a subpopulation of HCC expressing K19, a marker of biliary epithelium as well as stem/progenitor cell, is important to extrahepatic metastasis[38]. During this process, EMT is considered as a key component for metastasis[39]. However, the phenotypic change during metastasis and whether there are specific organotropic properties for metastatic organs have not been investigated.

When compared the morpho-phenotypical features of HCCs with those of extahepatic metastasis, they were generally conserved during extrahepatic metastasis. As EMT signature is one of important mechanism for initiation of metastasis, extrahepatic metastasis of HCCs is subgrouped into EMT-low (73.9%, 88/119) and EMT-high (26%, 31/119). Interestingly, EMT-low group exhibited higher incidence of VETC, less fibrous stroma and lower K19 expression, less immune cell infiltration and lower expression of PD-L1 by tumor and immune cells VETC compared to EMT-high group. According to organ with extrahepatic metastasis, VETC was most commonly found in lung, which is hematogenous spread, in contrast to no case of VETC in lymph node metastasis. In lymph node metastasis, it was clearly associated with EMT and K19 expression. It is consistent with the previous report that suggested VETC affects HCC metastasis by EMT-independent manner[24]. Taken together, the tumor characteristics of molecular feature and TME are considered to be closely involved in determining type of metastasis whether hematogenous or lymphatic invasion.

In conclusion, these data suggest the potential value of discerning VETC HCC, to predict aggressive behavior and optimize further the individual therapeutic approach.

V. CONCLUSION

The VETC phenotype (defined as ≥ 55% tumor area by CD34 immunostaining) was easily reproducible and reliably detectable vascular pattern. The VETC-HCCs were significantly associated with several clinical and pathological features and poorer prognosis. This distinct vascular pattern

was enriched in the macrotrabecular massive HCC subtype and β-catenin/Wnt activation.

In terms of TME, VETC-HCCs showed several conflicting features to non-VETC-HCCs with fibrous stroma: EMT-low, scarce fibrous stroma with less immune cell infiltration, low PD-L1 expression, and increased CAIX expression.

For extrahepatic metastases, pulmonary metastatic tumors were associated with MTM subtype with VETC-HCCs and nodal metastatic tumors were more likely to express stemness- and EMT- related markers and PD-L1. In analysis for matched pair of primary and metastasis, overall, various features of HCCs including VETC were conserved during metastasis.

This study suggests that VETC phenotype is a distinct aggressive subtype with CAIX expression, EMT-low TME, and may predict response to immune checkpoint inhibitors.

REFERENCES

1. Matsuda T, Marugame T, Kamo K, Katanoda K, Ajiki W, Sobue T. Cancer incidence and incidence rates in Japan in 2003: based on data from 13 population-based cancer registries in the Monitoring of Cancer Incidence in Japan (MCIJ) Project. Jpn J Clin Oncol 2009;39:850-8.
2. Torre LA, Bray F, Siegel RL, Ferlay J, Lortet-Tieulent J, Jemal A. Global cancer statistics, 2012. CA Cancer J Clin 2015;65:87-108.
3. Llovet JM, Zucman-Rossi J, Pikarsky E, Sangro B, Schwartz M, Sherman M, et al. Hepatocellular carcinoma. Nature Reviews Disease Primers 2016;2:16018.
4. Zucman-Rossi J, Villanueva A, Nault JC, Llovet JM. Genetic Landscape and Biomarkers of Hepatocellular Carcinoma. Gastroenterology 2015;149:1226-39.e4.
5. Chiang DY, Villanueva A, Hoshida Y, Peix J, Newell P, Minguez B, et al. Focal gains of VEGFA and molecular classification of hepatocellular carcinoma. Cancer Res 2008;68:6779-88.
6. Hoshida Y, Nijman SM, Kobayashi M, Chan JA, Brunet JP, Chiang DY, et al. Integrative transcriptome analysis reveals common molecular subclasses of human hepatocellular carcinoma. Cancer Res 2009;69:7385-92.
7. Boyault S, Rickman DS, de Reynies A, Balabaud C, Rebouissou S, Jeannot E, et al. Transcriptome classification of HCC is related to gene alterations and to new therapeutic targets. Hepatology 2007;45:42-52.
8. Lee JS, Heo J, Libbrecht L, Chu IS, Kaposi-Novak P, Calvisi DF, et al. A novel prognostic subtype of human hepatocellular carcinoma derived from hepatic progenitor cells. Nat Med 2006;12:410-6.
9. Toffanin S, Hoshida Y, Lachenmayer A, Villanueva A, Cabellos L, Minguez B, et al. MicroRNA-based classification of hepatocellular carcinoma and oncogenic role of miR-517a. Gastroenterology 2011;140:1618-28.e16.
10. Harding JJ, Nandakumar S, Armenia J, Khalil DN, Albano M, Ly M, et al. Prospective Genotyping of Hepatocellular Carcinoma: Clinical Implications of Next-Generation Sequencing for Matching Patients to Targeted and Immune Therapies. Clin Cancer Res 2019;25:2116-26.
11. Llovet JM, Montal R, Sia D, Finn RS. Molecular therapies and precision medicine for hepatocellular carcinoma. Nat Rev Clin Oncol 2018;15:599-616.
12. Sia D, Jiao Y, Martinez-Quetglas I, Kuchuk O, Villacorta-Martin C, Castro de Moura M, et al. Identification of an Immune-specific Class of Hepatocellular Carcinoma, Based on Molecular Features. Gastroenterology 2017;153:812-26.
13. Pinyol R, Sia D, Llovet JM. Immune Exclusion-Wnt/CTNNB1 Class Predicts Resistance to Immunotherapies in HCC. Clin Cancer Res 2019;25:2021-3.
14. Hanahan D, Weinberg RA. Hallmarks of cancer: the next generation. Cell 2011;144:646-74.
15. Bissell MJ, Radisky DC, Rizki A, Weaver VM, Petersen OW. The organizing principle: microenvironmental influences in the normal and malignant breast.

Differentiation 2002;70:537-46.
16. Poisson J, Lemoinne S, Boulanger C, Durand F, Moreau R, Valla D, et al. Liver sinusoidal endothelial cells: Physiology and role in liver diseases. J Hepatol 2017;66:212-27.
17. Ichida T, Hata K, Yamada S, Hatano T, Miyagiwa M, Miyabayashi C, et al. Subcellular abnormalities of liver sinusoidal lesions in human hepatocellular carcinoma. J Submicrosc Cytol Pathol 1990;22:221-9.
18. Roncalli M, Roz E, Coggi G, Di Rocco MG, Bossi P, Minola E, et al. The vascular profile of regenerative and dysplastic nodules of the cirrhotic liver: implications for diagnosis and classification. Hepatology 1999;30:1174-8.
19. Sciarra A, Di Tommaso L, Nakano M, Destro A, Torzilli G, Donadon M, et al. Morphophenotypic changes in human multistep hepatocarcinogenesis with translational implications. J Hepatol 2016;64:87-93.
20. Rudini N, Novello C, Destro A, Riboldi E, Donadon M, Vigano L, et al. Phenotypic and molecular changes in nodule-in-nodule hepatocellular carcinoma with pathogenetic implications. Histopathology 2018;73:601-11.
21. Naumov GN, Akslen LA, Folkman J. Role of angiogenesis in human tumor dormancy: animal models of the angiogenic switch. Cell Cycle 2006;5:1779-87.
22. Aguirre-Ghiso JA. Models, mechanisms and clinical evidence for cancer dormancy. Nat Rev Cancer 2007;7:834-46.
23. Faillaci F, Marzi L, Critelli R, Milosa F, Schepis F, Turola E, et al. Liver Angiopoietin-2 Is a Key Predictor of De Novo or Recurrent Hepatocellular Cancer After Hepatitis C Virus Direct-Acting Antivirals. Hepatology 2018;68:1010-24.
24. Fang JH, Zhou HC, Zhang C, Shang LR, Zhang L, Xu J, et al. A novel vascular pattern promotes metastasis of hepatocellular carcinoma in an epithelial-mesenchymal transition-independent manner. Hepatology 2015;62:452-65.
25. Fang JH, Xu L, Shang LR, Pan CZ, Ding J, Tang YQ, et al. Vessels That Encapsulate Tumor Clusters (VETC) Pattern Is a Predictor of Sorafenib Benefit in Patients with Hepatocellular Carcinoma. Hepatology 2018; doi:10.1002/hep.30366.
26. Uchino K, Tateishi R, Shiina S, Kanda M, Masuzaki R, Kondo Y, et al. Hepatocellular carcinoma with extrahepatic metastasis: clinical features and prognostic factors. Cancer 2011;117:4475-83.
27. Shiozawa Y, Nie B, Pienta KJ, Morgan TM, Taichman RS. Cancer stem cells and their role in metastasis. Pharmacology & therapeutics 2013;138:285-93.
28. Li S, Li Q. Cancer stem cells and tumor metastasis (Review). International journal of oncology 2014;44:1806-12.
29. Calderaro J, Couchy G, Imbeaud S, Amaddeo G, Letouze E, Blanc JF, et al. Histological subtypes of hepatocellular carcinoma are related to gene mutations and molecular tumour classification. J Hepatol 2017;67:727-38.
30. Ziol M, Pote N, Amaddeo G, Laurent A, Nault JC, Oberti F, et al. Macrotrabecular-massive hepatocellular carcinoma: A distinctive histological subtype with clinical relevance. Hepatology 2018;68:103-12.
31. Hendry S, Salgado R, Gevaert T, Russell PA, John T, Thapa B, et al. Assessing Tumor-infiltrating Lymphocytes in Solid Tumors: A Practical

Review for Pathologists and Proposal for a Standardized Method From the International Immunooncology Biomarkers Working Group: Part 1: Assessing the Host Immune Response, TILs in Invasive Breast Carcinoma and Ductal Carcinoma In Situ, Metastatic Tumor Deposits and Areas for Further Research. Adv Anat Pathol 2017;24:235-51.

32. Qu B, Liu BR, Du YJ, Chen J, Cheng YQ, Xu W, et al. Wnt/beta-catenin signaling pathway may regulate the expression of angiogenic growth factors in hepatocellular carcinoma. Oncol Lett 2014;7:1175-8.
33. Kurebayashi Y, Ojima H, Tsujikawa H, Kubota N, Maehara J, Abe Y, et al. Landscape of immune microenvironment in hepatocellular carcinoma and its additional impact on histological and molecular classification. Hepatology 2018;68:1025-41.
34. Calderaro J, Meunier L, Nguyen CT, Boubaya M, Caruso S, Luciani A, et al. ESM1 as a Marker of Macrotrabecular-Massive Hepatocellular Carcinoma. Clin Cancer Res 2019;25:5859-65.
35. Schmittnaegel M, Rigamonti N, Kadioglu E, Cassará A, Rmili CW, Kiialainen A, et al. Dual angiopoietin-2 and VEGFA inhibition elicits antitumor immunity that is enhanced by PD-1 checkpoint blockade. Science translational medicine 2017;9:eaak9670.
36. Wu FT, Lee CR, Bogdanovic E, Prodeus A, Gariépy J, Kerbel RS. Vasculotide reduces endothelial permeability and tumor cell extravasation in the absence of binding to or agonistic activation of Tie2. EMBO molecular medicine 2015;7:770-87.
37. Holopainen T, Saharinen P, D'Amico G, Lampinen A, Eklund L, Sormunen R, et al. Effects of angiopoietin-2-blocking antibody on endothelial cell-cell junctions and lung metastasis. J Natl Cancer Inst 2012;104:461-75.
38. Ding S-J, Li Y, Tan Y-X, Jiang M-R, Tian B, Liu Y-K, et al. From proteomic analysis to clinical significance: overexpression of cytokeratin 19 correlates with hepatocellular carcinoma metastasis. Molecular & Cellular Proteomics 2004;3:73-81.
39. Fabregat I, Malfettone A, Soukupova J. New insights into the crossroads between EMT and stemness in the context of cancer. Journal of clinical medicine 2016;5:37.

ABSTRACT (IN KOREAN)

종양 군집을 둘러싸는 혈관형 간세포암: 불량한 예후를 보이는 간세포암 아형

<지도교수 박 영 년>

연세대학교 대학원 의학과

우 하 영

간세포암은 전 세계에서 암 사망의 주요한 원인이다. 최근 간세포암에서 vessels encapsulating tumor cluster (VETC)라는 특이한 혈관 모양이 종양의 급격한 전파와 높은 재발율과 연관됨이 보고된 바 있으며, 이것은 CD34 면역염색에서 종양 군집을 혈관 내피세포가 동그랗게 둘러싸는 형태로 확인할 수 있다. 본 연구에서, 우리는 VETC의 임상 병리학적 특징을 규명하고, 특히 종양 미세 환경적 특징을 알아보고자 하였다.

본 연구는 2006년부터 2012년까지 세브란스 병원에서 수술적으로 절제된 원발성 간암 (코호트 1, 322례)과 간외 전이성 간암 (코호트 2, 130례) 조직을 대상으로 시행하였다. 각 종양에서 임상 및 병리학적 변수들 검색하였으며, 특히 종양의 섬유성 기질과 염증 세포 침윤을 반정량적으로 평가하였다. 면역 염색은 각각의 표지자로서 다음의 항목에 대하여 조직미세배열을 이용하여 시행하였다: CD34 (종양 혈관), αSMA, FAP (종양 섬유모세포), CD163 (제2형 종양 연관 대식세포), Zebl, Snail, Ezrin, S100A4, E-cadherin (상피-간엽 이행), PD-L1 (종양 면역), CAIX(저산소), K19 (종양 줄기세포), p53, glutamine synthetase, β-catenin (분자 아형).

VETC 값은 조직 미세 배열과 큰 조직 절편에서 양호한 일치율을

보였으며 (급내 상관계수=0.642), 관찰자간 재현성 또한 우수하였다 (코헨 카파계수=0.879). VETC 값은 불량한 무병 생존율 (HR: 1.04 [1.01-1.08]; p=0.006), 조기 재발율 (HR: 1.04 [1.01-1.08]; p=0.006), 전체 생존율 (HR: 1.06 [1.00-1.11]; p=0.041), 그리고 간외 전이 (HR: 1.06 [1.01-1.11]; p= 0.009)와 연관 있었다. K-adaptive partitioning algorithm을 통해 VETC (%)의 최적의 절사값을 구하여 VETC가 종양 면적의 55% 이상인 것을 VETC 아형으로 정의하였다. VETC 아형은 전체 증례 중 23.0% (74/322)이었으며, 높은 혈중 AFP (> 400 ng/ml)/PIVKA-II (> 300 mAU/mL) 농도, 종양 크기 5 cm 이상, 대혈관 침범, 나쁜 분화, 거대기둥 모양, 소혈관 침범, 다핵 종양세포과 연관이 있었다. 또한 VETC 아형은 조기 재발 (HR 1.91 [1.20-3.02]; p=0.006), 불량한 전체 생존율 (HR 2.84 [1.29-6.26]; p=0.010), 그리고 간외 전이 (HR 2.38 [1.21-4.64]; p=0.011)와 연관 있음이 다변량 분석에서 확인되었다. VETC 아형은 거대기둥형 간세포암과 분자적으로는 β-catenin/Wnt 활성화와 연관 있는 것으로 관찰되었다.

종양미세환경 측면에서, VETC아형은 상피-간엽 이행성이 낮고 섬유성 종양 기질 및 염증세포 침윤이 적고, PD-L1 발현이 낮고, 저산소성을 보였다. 반면 VETC가 아닌 간암 (non-VETC)의 종양미세환경은 다양한 소견을 보였으며, 섬유성 기질이 있는 경우 (117례), 섬유성 기질이 없는 경우 (131례)로 세분하였다. 이중 섬유성 종양 기질이 있는 non-VETC는 상피-간엽 이행적 특징과 K19 및 PD-L1 발현이 높고, 염증세포의 침윤이 풍부하였으며, 분자적으로는 p53(-), glutamine synthetase/β-catenin (-)이 많았다 (모두 $p<0.05$). 반면 섬유성 기질이 없는 non-VETC는 VETC 아형과 비교했을 때, K19과 PD-L1 발현 정도가 비슷하고 섬유성 기질이 있는 non-VETC에 비하여서는 p53 발현이 높았다 (모두 $p<0.05$). 생존 분석에서 VETC 환자군이 가장 불량한 예후를 보였고, 섬유성 기질이 없는 non-VETC 환자군이 최상의 예후를 보였으며, 섬유성 기질이 있는 non-VETC가

그 중간의 예후를 보였다.

간외로 전이된 간세포암은 원발성 간세포암에 비해 조직학적으로는 거대 기둥형이 더 많았고, 미세 환경적 측면에서는 저산소성, 상피-간엽 이행성, K19의 발현이 높았다 (모두 $p<0.05$). 간외로 전이된 간세포암을 상피-간엽 이행성 마커의 발현정도에 따라 나누면, 상피-간엽 이행성이 낮은 간외전이 그룹은 VETC와 연관이 있었고, 상피-간엽 이행성이 높은 간외 전이 그룹은 섬유성 종양기질이 풍부하고, K19 발현, 염증세포 침윤과 PD-L1 발현율이 높았다 (모두 $p< 0.05$). 간외 전이가 일어난 장기별 특성으로서 폐로 전이된 간암은 거대 기둥형 및 VETC 아형이 많았고, 림프절로 전이된 종양은 K19 및 상피-간엽 이행성 표지자의 발현이 높았다. 원발 간암과와 대응되는 간외 전이 간암의 비교에서, VETC를 포함하여 종양의 병리학적 특성은 대체로 유지되는 경향을 보였다.

본 연구는 VETC가 공격적인 생물학적 특성과 연관된 간세암종의 아형으로서 종양 미세환경적으로 상피-간엽 이행성이 낮고 섬유성 종양 기질 및 염증세포 침윤이 적고, PD-L1 발현이 낮고, 저산소성의 특성을 보였다. 또한 VETC 형태를 보이는 간외전이 간암에서는 상피-간엽 이행성이 낮으며, 폐로의 전이가 많은 특성을 보였다.

결론적으로 본 연구에서 VETC 아형은 불량한 예후 예측하며, 간암의 맞춤치료를 위한 표지자로서의 가능성을 제시하였다.

핵심되는 말 : 간세포암, 종양 군집을 둘러싸는 혈관, 종양 미세환경, 상피-간엽 이행, 간외 전이